

Effect of Paraffins on Carbon Dioxide Corrosion and Water Wetting in Oil-Water
Systems

A thesis presented to
the faculty of
the Russ College of Engineering and Technology of Ohio University

In partial fulfillment
of the requirements for the degree
Master of Science

Shanshan Yang

June 2010

© 2010 Shanshan Yang. All Rights Reserved.

This thesis titled
Effect of Paraffins on Carbon Dioxide Corrosion and Water Wetting in Oil-Water
Systems

by

SHANSHAN YANG

has been approved for
the Department of Chemical and Biomolecular Engineering
and the Russ College of Engineering and Technology by

Srdjan Nesic

Professor of Chemical and Biomolecular Engineering

Dennis Irwin

Dean, Russ College of Engineering and Technology

ABSTRACT

YANG, SHANSHAN, M.S., June 2010, Chemical Engineering

Effect of Paraffins on Carbon Dioxide Corrosion and Water Wetting in Oil-Water Systems (102 pp.)

Director of Thesis: Srdjan Nestic

Paraffins are one of the most common components in crude oil. Paraffin wax can generate corrosion inhibition by wax formation on the internal surface of the pipeline, reducing the corrosion. Furthermore, paraffin wax is believed to have effects on wettability of steel as well as the interfacial tension of oil and water, with consequent positive effect on the internal pipeline corrosion.

The objective of the study is to experimentally investigate the effect of paraffins on CO₂ corrosion rate, wettability and interfacial tension in an oil-water system. Furthermore, the goal was to develop a thermodynamic model to predict the wax appearance temperature (WAT) theoretically.

The corrosion inhibition measurements, contact angle measurements and interfacial tension measurements were conducted at two different temperatures, 30 °C (above the WAT) and 5 °C (below the WAT), using a synthetic paraffin-oil mixture which is composed of LVT200 and a laboratory grade n-paraffin called Eicosane [CH₃(CH₂)₁₈CH₃] at different concentration, ranging from 0 to 50 wt%. A model for predicting wax precipitation was proposed by applying thermodynamic principles, mass balances and computational methods.

It is found that paraffins produce significant corrosion inhibition at temperatures below the WAT. Paraffins change the wettability of steel surface from being hydrophilic to hydrophobic when the temperature is below the WAT. A new thermodynamic model for predicting wax precipitation was proposed and agrees rather well with experimental results for synthetic normal paraffin oils.

Approved: _____

Srdjan Nesic

Professor of Chemical and Biomolecular Engineering

ACKNOWLEDGEMENTS

I would like to express the deepest gratitude is to my advisor, Dr. Srdjan Nestic for his support, guidance and encouragement during my master study at Ohio University.

I would also like to express my sincere appreciation to my project leader, Dr. Sonja Richter for her leadership on my research project, Dr. Winston Robbins for his advice on paraffins study and Dr. Tingyue Gu for his suggestion on wax precipitation model.

I appreciate all the faculty, staff and my fellow students at Institute for Corrosion and Multiphase Technology for their support and advice throughout the project. I would like to give special mention to Dr. Chong Li and Mr. Xuanping Tang.

DEDICATION

To

My father, Jiguang Yang

and

My mother, Benhong Gong

TABLE OF CONTENTS

	Page
Abstract.....	3
Acknowledgements.....	5
Dedication.....	6
List of Tables	9
List of Figures.....	10
Chapter 1: Introduction.....	14
1.1 CO ₂ corrosion	16
1.2 Water wetting.....	19
1.3 Paraffins	20
Chapter 2: Experimental Setup and Procedures.....	24
2.1 Properties of the synthetic paraffin-oil mixture.....	25
2.1.1 Viscosity	26
2.1.2 Wax appearance temperature (WAT)	28
2.1.3 Density	30
2.2 Wax precipitation on the steel surface.....	30
2.3 Corrosion inhibition.....	34
2.3.1 Corrosion inhibition above the wax appearance temperature (WAT).....	37
2.3.2 Corrosion inhibition below the wax appearance temperature (WAT).....	38
2.3.3 Effect of shear on corrosion inhibition	41
2.3.4 Corrosion inhibition at a varying temperature	41
2.4 Wettability	42
2.5 Interfacial tension	47
Chapter 3: Results and Discussion.....	50
3.1 Properties of the synthetic paraffin-oil mixture.....	50
3.1.1 Viscosity	50
3.1.2 Wax appearance temperature (WAT)	51
3.1.3 Density	52
3.2 Wax precipitation on the steel surface.....	53

3.3 Corrosion inhibition	55
3.3.1 Corrosion inhibition above the wax appearance temperature (WAT)	55
3.3.2 Corrosion inhibition below the wax appearance temperature (WAT)	57
3.3.3 Effect of shear on corrosion inhibition	61
3.3.4 Corrosion inhibition at a varying temperature	63
3.4 Wettability	64
3.4.1 Oil droplet in water phase	65
3.4.2 Oil droplet in water phase (oil pre-wet specimen)	67
3.4.3 Water droplet in oil phase	71
3.4.4 Water droplet in oil phase (oil pre-wet specimen)	73
3.5 Interfacial tension	77
Chapter 4: Thermodynamic Model for Wax Precipitation	78
4.1 General solid-liquid equilibrium	79
4.2 Fugacities of pure substance for liquid and solid at the reference state	81
4.3 Activity coefficient model	83
4.4 Modeling calculation	87
4.5 Model validation	89
Chapter 5: Conclusions	96
References	97
Appendix A: Linear Polarization Resistance	101

LIST OF TABLES

	Page
Table 1: Chemical Composition of Carbon Steels (X65 and C1018).....	15
Table 2: Test Matrix Showing the Concentration of the Synthetic Paraffin-Oil Mixture	26
Table 3: Properties of Falling Balls Accompanying with Viscometer	28
Table 4: Test Matrix for Wax Precipitation Measurement	33
Table 5: Test Matrix for Corrosion Inhibition Measurement	36
Table 6: Test Matrix for Contact Angle Measurement.....	45
Table 7: 4 Sets of Experiments for Wettability Measurement.....	45
Table 8: Test Matrix for Interfacial Tension Measurement.....	48
Table 9: Values of Solubility Parameters for Normal Paraffins	85
Table 10: Composition of the Synthetic Oil Mixtures Used to Test the Model	90
Table 11: Comparison of the WAT between Experimental and Model Results.....	93

LIST OF FIGURES

	Page
Figure 1: Solid Eicosane at room temperature.....	25
Figure 2: Setup of the Haake viscometer used to measure the viscosity of the synthetic paraffin-oil mixture	27
Figure 3: Setup for measuring the wax appearance temperature (WAT)	29
Figure 4: Peltier cooler.....	31
Figure 5: Configuration of cooling apparatus used for measurement of wax precipitation on the steel surface	32
Figure 6: Setup for measurement of wax precipitation on the steel surface	33
Figure 7: Three electrode glass cell setup using the rotating cylinder as the working electrode, silver/silver-chloride (Ag/AgCl) as the reference electrode and the platinum ring as the counter electrode	35
Figure 8: Sketch of the contact angle, θ , of (a) water droplet (water-in-oil) (b) oil droplet (oil-in-water)	43
Figure 9: Goniometer setup with the video camera and a backlight.....	44
Figure 10: Test cell of goniometer with a carbon steel (X65) specimen on the specimen holder.....	44
Figure 11: Setup of tensiometer using a platinum ring to measure the interfacial tension between water and oil.....	48
Figure 12: Viscosity of the synthetic paraffin-oil mixture at the ambient temperature. 51	
Figure 13: Wax appearance temperature (WAT) of the synthetic paraffin-oil mixture.52	

Figure 14: Density of the synthetic paraffin-oil mixture at the ambient temperature	53
Figure 15: Weight of wax precipitation as a function of time and oil temperature. (Oil source: 30 wt% synthetic paraffin-oil mixture. Specimen temperature: 5 °C.)	54
Figure 16: LPR results of 3 steps of corrosion inhibition measurement for the synthetic paraffin-oil mixture at 30 °C (above the WAT).....	56
Figure 17: LPR results of the partitioning step for the synthetic paraffin-oil mixture at 5 °C (below the WAT)	58
Figure 18: LPR results of the corrosion inhibition and persistency step for Procedure 1 at 5 °C (below the WAT)	59
Figure 19: LPR results of the corrosion inhibition and persistency step for Procedure 2 at 5 °C (below the WAT). (Oil source: 30 wt% synthetic paraffin-oil mixture. Specimen temperature: 5 °C.)	60
Figure 20: LPR results for testing the effect of shear on corrosion inhibition	62
Figure 21: LPR results for testing the effect of shear on corrosion inhibition	63
Figure 22: LPR results for testing the effect of increasing the temperature from 5 °C to 30 °C on corrosion inhibition	64
Figure 23: Droplets of the synthetic paraffin-oil mixture on the surface of carbon steel (X65) in 1 wt% NaCl aqueous solution (water) phase at 30 °C.....	65
Figure 24: Droplet of LVT200 on the surface of carbon steel (X65) in 1 wt% NaCl aqueous solution (water) phase at 5 °C	66

- Figure 25: Contact angle measurements of the droplets of the synthetic paraffin-oil mixture in 1 wt% NaCl aqueous solution (water) phase at 5 °C and 30 °C67
- Figure 26: Droplets of the synthetic paraffin-oil mixture in 1 wt% NaCl aqueous solution (water) phase at 30 °C on the surface of carbon steel (X65) which is pre-wetted with the synthetic paraffin-oil mixture.....68
- Figure 27: Droplets of LVT200 in 1 wt% NaCl aqueous solution (water) phase at 5 °C on the surface of carbon steel (X65) which is pre-wetted with the synthetic paraffin-oil mixture69
- Figure 28: Contact angle measurements of the droplets of the synthetic paraffin-oil mixture in 1 wt% NaCl aqueous solution (water) phase at 5 °C and 30 °C on the surface of carbon steel (X65) which is pre-wetted with the synthetic paraffin-oil mixture70
- Figure 29: Water droplets on the surface of the carbon steel (X65) surface in the synthetic paraffin-oil mixture at 30 °C71
- Figure 30: Water droplets on the surface of the carbon steel (X65) surface in LVT200 oil phase at 5 °C72
- Figure 31: Contact angle measurements of water droplets in the synthetic paraffin-oil mixture at 5 °C and 30 °C.....73
- Figure 32: Water droplets in the synthetic paraffin-oil mixture at 30 °C on the surface of carbon steel (X65) which is pre-wetted with the synthetic paraffin-oil mixture74

Figure 33: Water droplet in LVT200 oil phase at 5 °C on the surface of carbon steel (X65) which is pre-wetted with the synthetic paraffin-oil mixture	75
Figure 34: Contact angle measurements of water droplets in the synthetic paraffin-oil mixture at 5 °C and 30 °C on the surface of carbon steel (X65) which is pre-wetted with the synthetic paraffin-oil mixture	76
Figure 35: Interfacial tension measurements between the synthetic paraffin-oil mixture and 1 wt% NaCl aqueous solution at 30 °C	77
Figure 36: Procedure chart of the calculation of thermodynamic model for wax precipitation.....	89
Figure 37: Experimental and predicted wax precipitation results for synthetic Mixture A	91
Figure 38: Experimental and predicted wax precipitation results for synthetic Mixture B	91
Figure 39: Experimental and predicted wax precipitation results for synthetic Mixture C	92
Figure 40: Wax precipitation results: experiments and new model conducted by adjusting the ratio of activity coefficient for Mixture A.....	94
Figure 41: Wax precipitation results: experiments and new model conducted by adjusting the ratio of activity coefficient for Mixture B	95
Figure 42: Wax precipitation results: experiments and new model conducted by adjusting the ratio of activity coefficient for Mixture C	95

CHAPTER 1: INTRODUCTION

In petroleum reservoirs, crude oil is accompanied by natural gas, formation water, mineral salts and a variety of other components, including some corrosive species. These materials are produced in the so called “upstream” operations (wells, pipelines, etc.), and then transported to the processing facilities (for separation, refining, etc.) – the so called “downstream” facilities. In order to boost the reservoir pressure, the separated formation water is often re-injected back into the petroleum reservoirs (sometimes mixed with seawater). Therefore, the produced water may continuously accumulate in oilfield reservoir over the years. Due to the existence of water and corrosive species, the internal corrosion of transportation pipelines may occur. Economic factors rule out use of corrosion resistant alloys (CRAs) due to the high cost. Therefore, due to low cost, easy manufacturing and convenient utilization, carbon steel is used extensively. Table 1 shows the chemical composition of two types of common carbon steels. However, the lifetime of carbon steel pipelines is limited by internal corrosion. A recent study performed by NACE International (Cost of Corrosion, 1998) estimated that the cost of corrosion in the United States is \$276 billion annually including \$138 billion of direct cost. A large portion of that is related to corrosion in transportation utilities with internal corrosion of pipelines playing a significant role. Therefore, in order to reduce the loss caused by internal corrosion, it is necessary to understand the phenomena of internal pipeline corrosion better and qualify the factors that affect it.

Table 1. *Chemical Composition of Carbon Steels (X65 and C1018) (wt%)*

	C	Si	P	S	Mn	Al	Cr	Cu	Ni	Fe
X65	0.14	0.25	0.013	0.004	1.16	0.031	0.15	0.14	0.38	balance
C1018	0.2	0.25	0.009	0.012	0.87	0.022	0.1	0.083	0.071	balance

Phase wetting regimes are believed to have a relationship with internal pipeline corrosion. When the corrosive water phase comes in contact with the internal surface of the carbon steel pipeline, water wetting occurs, leading to internal corrosion. On the contrary, oil wetting occurs when water is entrained in the oil phase, which means that the oil phase is in contact with the internal surface of the pipeline. In this case, if water is fully entrained in the oil phase, internal corrosion can be avoided. Two factors are believed to affect phase wetting. One is the wettability of the steel surface. If the steel surface is hydrophilic, the water phase will be more readily contacting with the pipeline surface, causing water wetting and eventually internal corrosion. Otherwise, when the steel surface is hydrophobic, oil is more readily in contact with the steel surface, and oil wetting occurs, leading to corrosion-free conditions. Normally, the wettability of the carbon steel surface is hydrophilic. Another factor is the interfacial tension between oil and water. At lower interfacial tension, water is more easily entrained by the oil phase, leading to oil wetting and less likelihood of internal corrosion. Therefore, it is important to study the relationship between internal pipeline corrosion and phase wetting and how to take advantage of phase wetting in order to prevent internal pipeline corrosion.

Paraffins are one of the most common components in crude oil. In chemistry, paraffin is the common name for alkane hydrocarbons with the general formula C_nH_{2n+2} .

The solid form of paraffin is usually called “paraffin wax” or just “wax”. Wax can precipitate and deposit on the internal pipe surface when oil containing paraffins comes in contact with the pipe wall at a temperature below the wax appearance temperature (WAT) of the paraffins. The thickness of the wax layer increases with time, which means that wax can accumulate on pipeline surface continuously if the temperature stays below the WAT. This characteristic of paraffins may cause blockage in the pipeline, thus significantly causing restriction in flow and leading to economic losses. However, wax deposits can promote corrosion inhibition by formation of wax layers on the internal pipeline surface and hinder access of the corrosive water to the pipeline surface, reducing the loss of metal due to corrosion. Moreover, paraffins are believed to have an effect on the wettability of the steel surface and the interfacial tension at the oil-water interface. Both are believed to affect internal pipeline corrosion significantly.

The objective of the study is to experimentally investigate the effect of paraffins on CO₂ corrosion rate, wettability and interfacial tension in oil-water two-phase system as well as to predict the WAT theoretically.

1.1 CO₂ corrosion

In the petroleum industry, oil and water are usually transported together over a long distance in a pipeline. The presence of water in pipelines may cause serious internal corrosion, because it can dissolve corrosive gases such as carbon dioxide (CO₂). Dissolving carbon dioxide gas in the water will result in the formation of carbonic acid, causing acid corrosion of carbon steel. Although carbon dioxide corrosion can be avoided

by corrosion resistant alloys (CRAs), carbon steel is still extensively used for pipeline material due to the high cost of CRAs. Thus, it is important to know the theory of carbon dioxide corrosion on carbon steel. The basic mechanism of carbon dioxide corrosion has been studied comprehensively and widely accepted. The present research focuses on the effect of paraffins on the carbon dioxide corrosion inhibition building on the accepted carbon dioxide corrosion theory. Nordsveen *et al.* (2003) and Netic (2007) proposed that several chemical and electrochemical reactions occur in carbon dioxide corrosion.

As a first “step”, carbon dioxide dissolves in water (Equation (1)). The solubility of carbon dioxide is about 90 cm³ of CO₂ per 100 ml water and the proportion of aqueous carbon dioxide and gaseous carbon dioxide is 0.8 at room temperature (Reid *et al.*, 1987).

Next, equilibrium is established between the aqueous carbon dioxide and carbonic acid. The chemical reaction equilibrium constant of Equation (2) is 1.7×10^{-3} at room temperature and atmospheric pressure (Reid *et al.*, 1987), which indicates that only a small fraction of the aqueous CO₂ is actually converted to H₂CO₃. Thus, the corrosive carbonic acid is constantly being replenished as it is consumed by corrosion since there is a vast reservoir of gaseous and aqueous carbon dioxide.



Carbonic acid is a weak acid and can dissociate to form bicarbonate, carbonate and hydrogen ions in the following two steps:



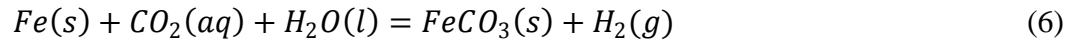
In corrosion iron dissolves and forms iron (ferrous) ions (Fe^{2+}). Solid iron carbonate ($FeCO_3$) can be formed on the steel surface when the concentration of Fe^{2+} and CO_3^{2-} exceed the solubility limit.



Fe^{2+} can be oxidized to form Fe^{3+} . However, because the water used in this research program is deoxygenated by purging carbon dioxide, Fe^{3+} does not form and hence is not considered.

The electrochemical processes occurring at the steel surface in CO_2 corrosion are as follows:

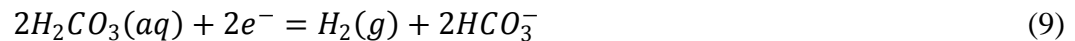
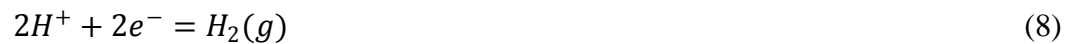
The overall reaction is given by:



The main anodic reaction is the dissolution of iron to give ferrous ions:



It is often assumed that the main cathodic reactions include direct proton reduction and direct carbonic acid reduction:



The occurrence of these two cathodic reactions depends on the corrosion environment, such as the pH. The general rule is that Equation (8) is dominant when $pH < 4$ while Equation (9) will dominate at a higher pH and high partial pressures of CO_2 .

Many environmental parameters, which can affect the carbon dioxide corrosion, have been studied. These parameters include pH, temperature, flow velocity, partial

pressure of carbon dioxide, water chemicals and oil chemicals (Nordsveen *et al.*, 2003; Nesic, 2007).

1.2 Water wetting

The surface of pipeline can corrode when the water phase comes physically in contact with the pipeline surface (water wetting) in the presence of carbon dioxide. On the contrary, this phenomenon will not occur when the oil phase is in contact with the pipeline surface (oil wetting) (Cai *et al.*, 2005). Hence the internal carbon dioxide corrosion is usually not problematic at a high flow rate of oil and/or low water cut when the water is entrained by the oil phase. Besides the flow rate and water cut, other factors such as crude oil chemicals, water chemicals, the wettability of the pipe surface, interfacial tension of the oil-water interface, and additives, etc. are also important for water wetting and pipeline internal corrosion (Li *et al.*, 2006). Water wetting is studied in two aspects in this research: the wettability of the steel surface and the interfacial tension at the oil-water interface. Contact angle is a good measure of the wettability of a steel surface (Rosen, 2004). Contact angle of an oil/water droplet is defined as the angle between the oil-water interface and the solid substrate line in contact with the water phase. A lower contact angle indicates hydrophilic surface and a high contact angle indicates hydrophobic surface. The contact angle is determined by the molecular attractive forces within each phase and between the phases.

Due to the hydrophobic (nonpolar) nature of oil molecules and the polar nature of water molecules, an interface can form between oil and water. At the oil-water interface,

adhesion occurs when the molecules of one phase attract the molecules of the other phase, while cohesion occurs when the molecules within the same phase interact among themselves. The interfacial tension is a measure of the competition of adhesion and cohesion (Berg, 1993). A lower interfacial tension lowers the threshold for which water is entrained in the oil phase, consequently causing that water is more easily entrained in oil phase. Oil wetting and less chance of internal corrosion are more easily to be achieved. In flowing oil-water system, it reflects as a dispersed flow pattern in which water is fully entrained in oil. On the contrary, a higher interfacial tension indicates water and oil are more easily to be separated, resulting in water wetting and stratified flow pattern (Li *et al.*, 2006). The effect of these two factors has been studied in a qualitative manner in the present research.

Based on the work done in the past, a generic water wetting model (Cai *et al.*, 2004) has been proposed and developed in the Water Wetting Joint Industry Project (WW-JIP) at the Institute for Corrosion and Multiphase Technology (ICMT) at Ohio University. Besides the pipeline diameter and inclination, oil density and viscosity, this model also takes into account oil-water interfacial tension and contact angle. Therefore, the study of interfacial tension and contact angle is important for understanding of water wetting.

1.3 Paraffins

In recent years, the effect of crude oil chemicals on CO₂ corrosion in oil-water flow has been investigated. In 1989, Efird *et al.* found that crude oil can generate

corrosion inhibition. It has been suggested that some crude oil chemicals can form a protective film on the pipeline surface and hence have an inhibition effect on corrosion in oil water flows (Cai *et al.*, 2005). Hernandez *et al.* (2005) also pointed out that crude oil has an impact on corrosion inhibition in oil-water flow pipeline due to the presence of crude oil components such as saturates and asphaltenes. dos Santos *et al.*, (2005) investigated the roles of the crude oil polar components including asphaltenes and naphthenic acids on the wetting by contact angle measurements and found by removing the polar components such as asphaltenes and naphthenic acids in crude oil, the steel surface can be changed from oil wetting to water wetting. In addition, Ajmera (2009) also found that some crude oil components (asphaltenes) have an effect on corrosion inhibition and wettability of steel surface.

Paraffins are one of the most common chemicals in crude oils. There are different definitions for paraffins. According to Speight (1998), paraffins are saturated hydrocarbons with straight (normal paraffins) or branched (isoparaffins) chains, but without any ring structure. Depending on the relative fraction of these compounds, a crude oil can be called paraffinic or naphthenic crude. Paraffinic petroleum may contain up to 20-50 wt% normal paraffins in the gas oil fraction (Speight, 1998). One of the most important concepts in understanding the characteristic of paraffins is the wax appearance temperature (WAT), which is the temperature at which a wax-oil mixture becomes a saturated solution (Singh *et al.*, 2000). It is necessary to predict precisely the WAT before oil production and transportation. Several thermodynamic models for predicting wax precipitation have been proposed previously. The models can be divided into two

categories: one which uses an equation of state and activity coefficients approach; the other is the two-equation of state approach. Both approaches employ equation of state for vapor-liquid equilibria (VLE). But for the liquid-solid equilibria (LSE), the former one uses an activity coefficient model (Won, 1986; Hansen *et al.*, 1988; Pederson *et al.*, 1991), while the latter one employs the equation of state (Lira-Galeana *et al.*, 1996; Ji *et al.*, 2003). In this research work, the first approach, equation of state plus activity coefficients, is applied and elaborated in Chapter 4.

Morales *et al.* (2000) suggested that the presence of paraffin wax promotes a significant reduction of corrosion rates according to the experimental data. However, the current understanding of the effect of paraffins on wetting is not sufficient. To investigate the effect of paraffins on wetting, one can measure contact angles of water and oil droplets on the steel surface. Also, interfacial tension is measured to understand if there is an effect of paraffins on the interfacial tension of water and oil which affects the flow pattern.

In order to study the effect of paraffins on carbon dioxide corrosion and wettability, the following experimental and modeling objectives have been formulated:

- Investigate the effect of paraffins on carbon dioxide corrosion inhibition in oil-water system at a temperature “above the WAT” and “below the WAT”.
- Study the impact of paraffins on the wettability of metal surface at a temperature “above the WAT” and “below the WAT”.
- Study the effect of paraffins on the interfacial tension between oil and water affecting the flow pattern.

- Predict the WAT by building a thermodynamic model for wax precipitation.
- Predict the amount of wax precipitation at a given temperature using a thermodynamic model for wax precipitation.

CHAPTER 2: EXPERIMENTAL SETUP AND PROCEDURES

This chapter covers experimental setups and procedures for five types of measurements: the properties of the synthetic paraffin-oil mixture, wax precipitation on the steel surface, corrosion inhibition, wettability (contact angle) and interfacial tension. Also, test matrices are included for each measurement series.

Due to the fact that a vast variety of components exist in the crude oil, it is not wise to study the effect of paraffins using a crude oil. So a synthetic paraffin-oil mixture was used to isolate the effect of paraffins. The synthetic paraffin-oil mixture is composed of LVT200 model oil and a laboratory grade normal paraffin (n-paraffin) called Eicosane [$\text{CH}_3(\text{CH}_2)_{18}\text{CH}_3$] at different concentrations. With melting point of 35 °C, Eicosane is solid crystal at room temperature. The morphology of Eicosane is shown in *Figure 1*. LVT200 was chosen to be the solvent for Eicosane because it is a paraffinic oil. LVT200 is made up from light hydrotreated petroleum distillates which consist of hydrocarbons in the range of C9 to C16 (MSDS provided by Penreco Company, see list of references). In addition, LVT200 is colorless, odorless, and its components do not precipitate even at a very low temperature (below 0 °C). Hence only Eicosane would precipitate when the temperature was below the WAT. Also, it is well known that LVT200 does not affect the corrosion rate or the wettability of the steel surface (Li *et al.*, 2006). Therefore, LVT200 is a good choice for solvent of Eicosane.

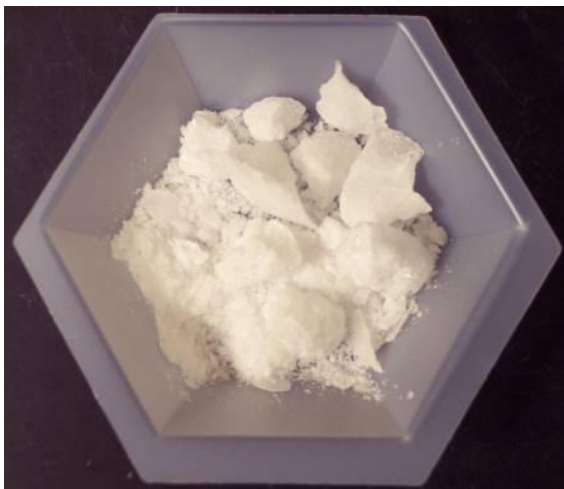


Figure 1. Solid Eicosane at room temperature.

2.1 Properties of the synthetic paraffin-oil mixture

In order to investigate the effect of paraffins, it is necessary to know the physical properties of a synthetic paraffin-oil mixture, including viscosity, wax appearance temperature (WAT) and density, because we need to establish if the properties of the synthetic paraffin-oil mixture are similar to a real crude oil and how by adding the Eicosane in the LVT200 these properties will be changed. Also, the knowing the WAT proved to be useful in the subsequent studies: of wax precipitation on the steel surface, corrosion inhibition, wettability and interfacial tension. The test matrix is shown in Table 2.

Table 2. Test Matrix Showing the Concentration of the Synthetic Paraffin-Oil Mixture

Parameter	Conditions
Paraffin source	Eicosane
Oil solvent	LVT200
Paraffin concentration	0, 10, 30, 50 wt% Eicosane in oil solvent

The concentration of Eicosane in the oil solvent is calculated using Equation (10).

$$C = \frac{m_{\text{Eicosane}}}{m_{\text{Eicosane}} + m_{\text{LVT 200}}} \times 100\% \quad (10)$$

where C is the concentration of Eicosane in LVT200 oil solvent, m_{Eicosane} is the mass of Eicosane and $m_{\text{LVT 200}}$ is the mass of LVT200 oil solvent in kg.

2.1.1 Viscosity

The viscosity was tested using a Haake viscometer (*Figure 2*) at an ambient temperature by means of a falling ball. The principle is based on Stoke's law for a sphere falling in a viscous fluid under the effect of gravity. Viscosity which has a unit of centipoise (cP) is a measure of the internal resistance of fluid to flow motion.

As seen in *Figure 2*, the circulating water jacket of the viscometer was connected to temperature-controlled bath to maintain the test liquid to the desired temperature. The measurement was made by taking the time it took the ball to fall between two set marks in the column filled with the testing fluid.

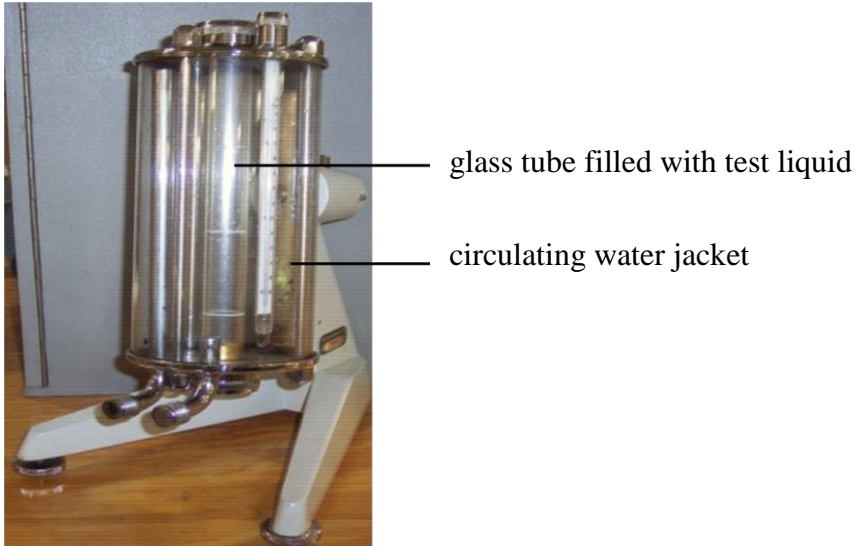


Figure 2. Setup of the Haake viscometer used to measure the viscosity of the synthetic paraffin-oil mixture.

An appropriate ball was chosen from the 6 balls listed in Table 3 according to the properties of the testing liquid. A general rule is to choose the ball which falls at a moderate speed in the testing liquid. The ball was placed in the glass tube filled with synthetic paraffin-oil mixture, and the time required for the steel ball to fall pass specified marks was recorded. For a given testing liquid, the viscosity depends on the falling time based on the following expression:

$$\mu = t(\rho_b - \rho_f)K \quad (11)$$

where μ is viscosity (cP), t represents ball's falling time (s), ρ_b is the density of ball (g/cm^3), ρ_f is the density of test fluid (g/cm^3) and K is ball constant which is given in Table 3 for each ball.

Table 3. *Properties of Falling Balls Accompanying with Viscometer*

	Diameter (mm)	Mass (g)	Density (g/cm³)	K
1	15.81	4.590	2.217	0.00834
2	15.65	4.445	2.216	0.0652
3	15.63	16.281	8.149	0.0815
4	15.22	15.050	8.141	0.613
5	14.29	11.798	7.706	4.51
6	11.12	5.554	7.717	33.5

The detailed procedure for testing viscosity is as follows:

1. Clean the viscometer tube with LVT200 oil, followed by alcohol and deionized water. Blow-dry the tube until it is dry.
2. Fill the viscometer tube halfway with the testing liquid. Insert the ball and fill up the tube full.
3. Turn the tube upside down and use a stopwatch to record the time for the ball to fall through marks, which are set 100mm apart.
4. Repeat the experiment by turning the tube over again 3-5 times.
5. Calculate the viscosity μ using equation (11), and find the mean and the standard deviation.

2.1.2 Wax appearance temperature (WAT)

Based on the objective related to studying the effect of paraffins at a temperature “below WAT” and “above WAT”, the WAT for synthetic paraffin-oil mixture should be determined first. The wax appearance temperature (WAT) was tested using an apparatus including an ice bath and a thermocouple (*Figure 3*). Synthetic paraffin-oil mixture

contained in beaker was placed in the ice bath, and the WAT recorded with the thermocouple as the temperature at which the first crystals were visually observed in the synthetic paraffin-oil mixture.

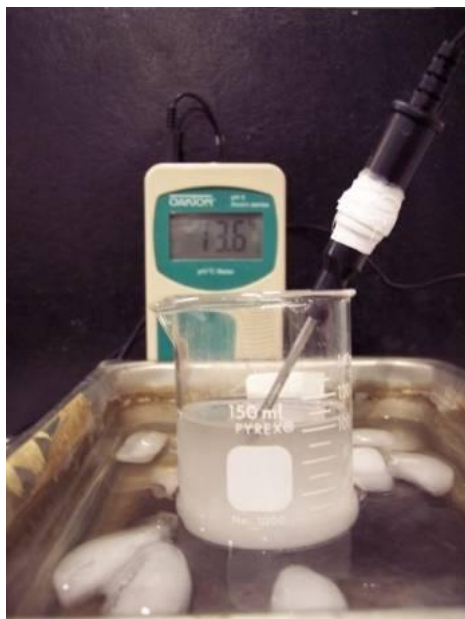


Figure 3. Setup for measuring the wax appearance temperature (WAT).

The test procedure is described below.

1. Heat the synthetic paraffin-oil mixture in a beaker to 35 °C.
2. Put the beaker in the ice bath, which consists of ice cubes in a tray filled with water.
3. Agitate the mixture until the first crystals are observed visually, and record the temperature on the thermocouple. This is the WAT. This cooling process had to be conducted slowly to avoid the mixture being over cooled. (It takes 30-40 minutes to cool from 35 °C to 0 °C for a 50ml mixture.)

4. Repeat the experiment over again 3-5 times and record the mean value and the standard deviation.

2.1.3 Density

Generally, crude oils can be classified as light, medium and heavy according to their density. Light crude oil is defined as having a density lower than 0.83 g/cm^3 and heavy oil is defined as having a density higher than 0.93 g/cm^3 .

A balance and a 100 ml graduated cylinder were employed to measure the density of synthetic paraffin-oil mixture.

The procedure for measuring the density is as follows.

1. Weigh an empty 100 ml graduated cylinder, m_1 (g).
2. Add synthetic paraffin-oil mixture into the cylinder and read the volume, V (ml).
3. Weigh the cylinder with the oil, m_2 (g).
4. Calculate the density of the synthetic paraffin-oil mixture as follows.

$$\rho_{Oil} = \frac{m_2 - m_1}{V} (\text{g/cm}^3) \quad (12)$$

5. Repeat this experiment over again 3-5 times and record the mean value and the standard deviation.

2.2 Wax precipitation on the steel surface

Crude oil is often transported to oil treatment facilities across cold environments such as arctic areas or ocean bottom. Given a temperature difference between the oil and the externally chilled pipe wall, wax can precipitate on inner pipeline surface. Wax

precipitation can accumulate on the pipeline surface gradually to form a thick layer, eventually causing the blockage of pipeline.

In order to study the effect of oil temperature on wax precipitation, a Peltier cooler (*Figure 4*) was employed. A Peltier cooler is a solid-state heat transfer device which transfers heat from one side (cold side) of the device to the other side (hot side) against the temperature gradient, with consumption of electrical energy. The effectiveness of the Peltier cooler depends on the amount of electrical energy provided and how well the heat can be removed from the hot side. *Figure 5* shows the configuration of a cooling apparatus used for this measurement. As seen in *Figure 5*, the bottom of Peltier cooler is the cold side for cooling specimen holder with an embedded thermistor and the mild steel specimen itself. The top of the Peltier device is the hot side. A heat sink is used to increase the surface area of heat released on the hot side to increase the efficiency of the Peltier cooler. The Peltier cooler is connected to a temperature controller which makes the temperature of specimen constant by adjusting the electrical energy input.

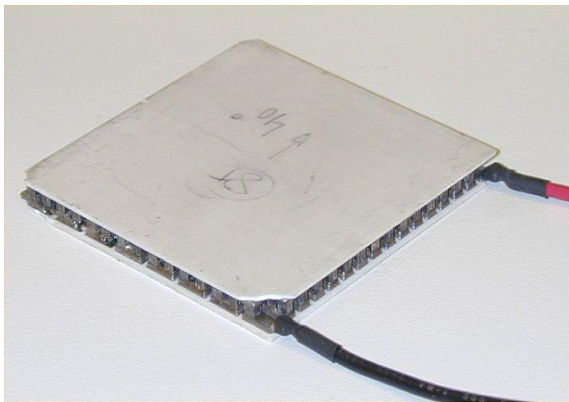


Figure 4. Peltier cooler. (Wikipedia)

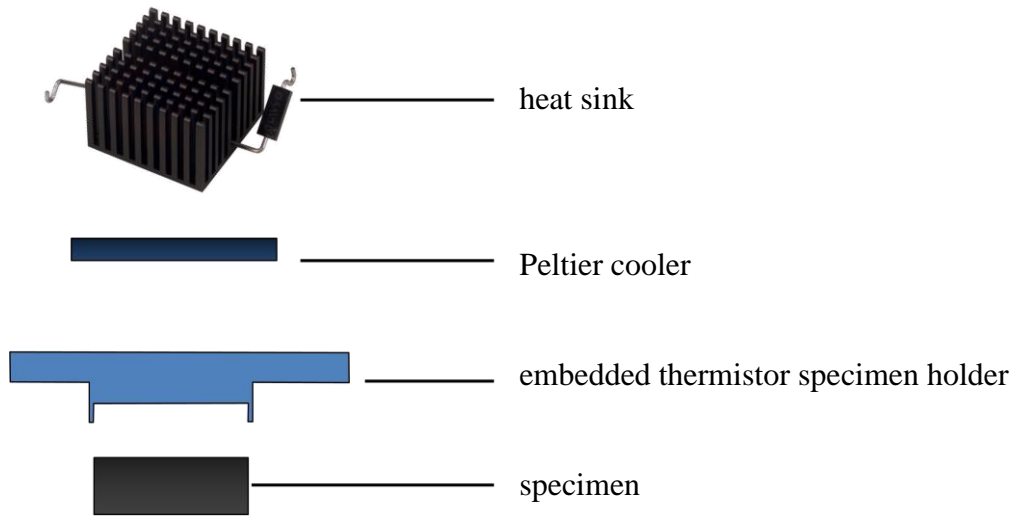


Figure 5. Configuration of cooling apparatus used for measurement of wax precipitation on the steel surface. (courtesy of Thunyaluk Pojtanabuntoeng)

Figure 6 shows the setup for testing wax precipitation on the steel surface. The beaker contained the synthetic paraffin-oil mixture at high temperature which is shown in Table 4. When the cold specimen came in contact with hot oil, wax precipitation occurred on the surface of steel specimen surface.

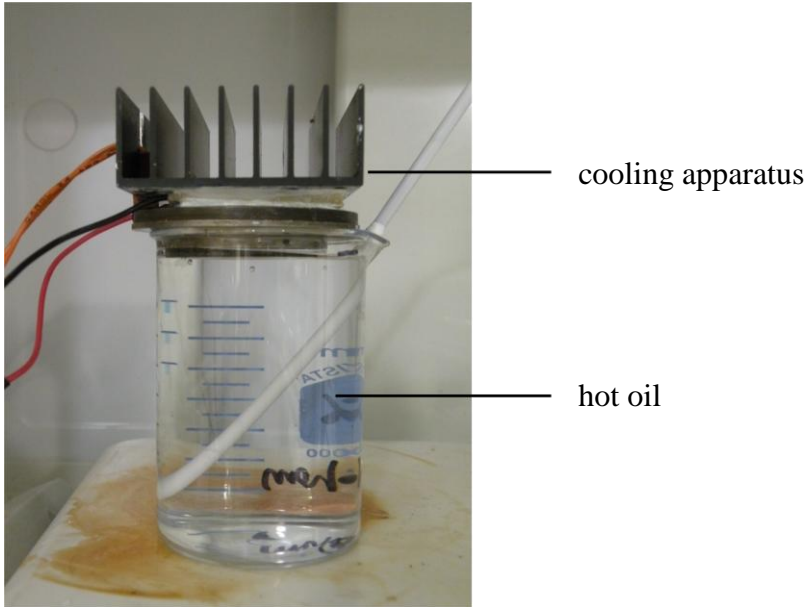


Figure 6. Setup for measurement of wax precipitation on the steel surface.

The test matrix for the wax precipitation on the steel surface is shown in Table 4.

Table 4. Test Matrix for Wax Precipitation Measurement

Parameter	Conditions
Specimen material	Carbon steel X65
Oil source	Synthetic paraffin-oil mixture (30 wt% Eicosane)
Oil temperature	20, 30, 40 °C
Specimen temperature	5 °C
Temperature difference (ΔT)	15, 25, 35 °C
Specimen surface area	8 cm ²

ΔT is the temperature difference between the cold specimen and the hot oil.

The detailed procedure for this measurement is shown as follows:

1. Polish the specimen with 600 grit silicon carbide paper, weigh it and put it on the specimen holder with the embedded thermistor.
2. Turn on the temperature controller and set temperature to 5 °C.
3. Heat the beaker containing the oil to the desired temperature (Table 4).
4. After the temperature of the specimen and the oil reached the desired temperatures and remained stable, immerse the specimen surface into the oil (*Figure 6*). The wax layer formed due to temperature difference between the cold specimen and hot oil.
5. Remove the specimen from the cooling apparatus and weigh it again.
6. The difference between two weights (before and after) is the weight of the wax.
7. Repeat this experiment 3-5 times and record the mean value and the standard deviation.

2.3 Corrosion inhibition

A glass cell (*Figure 7*) using three electrodes: a rotating cylinder as the working electrode, a silver/silver-chloride (Ag/AgCl) saturated with 1 M KCl solution as the reference electrode and a concentric platinum ring as the counter electrode, was used to perform the corrosion inhibition measurement. Linear polarization resistance (LPR) technique was used to measure the corrosion rate using a Gamry potentiostat. The principles of LPR are explained in Appendix A.

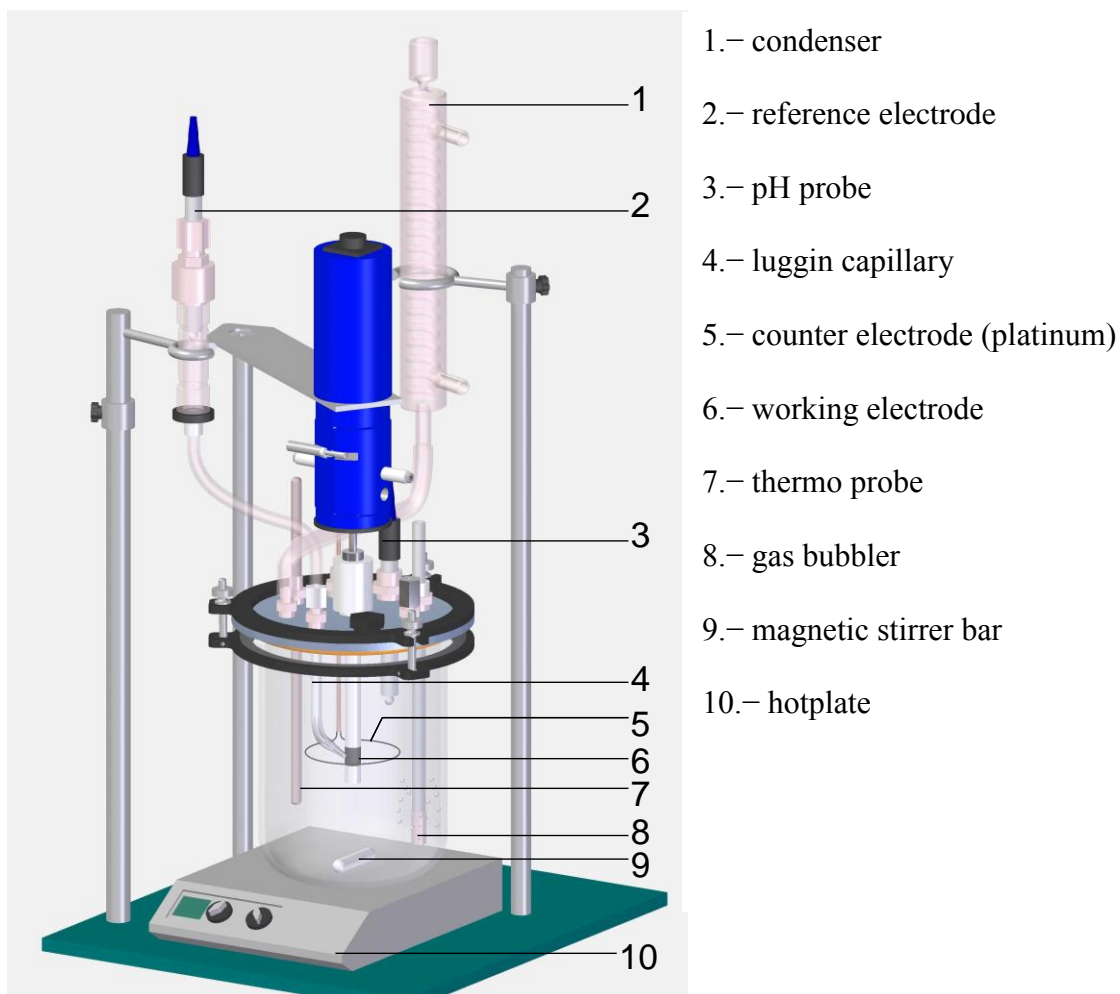


Figure 7. Three electrode glass cell setup using the rotating cylinder as the working electrode, silver/silver-chloride (Ag/AgCl) as the reference electrode and the platinum ring as the counter electrode. (courtesy of Haitao Fang)

Table 5 shows the test matrix for the corrosion inhibition measurements which were performed in a glass cell.

Table 5. Test Matrix for Corrosion Inhibition Measurement

Parameter	Conditions
Electrochemical technique	Linear Polarization Resistance (LPR)
Oil phase	Synthetic paraffin-oil mixture
Water phase	1 wt% NaCl aqueous solution
Specimen material	Carbon steel (X65)
Specimen surface area	5.4 cm ²
CO ₂ partial pressure	0.96 bar
Total pressure	1 bar
pH	5
Temperature	5 °C (below WAT), 30 °C (above WAT)
Rotation speed	1000 rpm

Initially, the glass cell including the Ag/AgCl reference electrode and the platinum counter electrode was filled with 1.75 L of 1wt% NaCl aqueous solution, where this test solution was deoxygenated by purging it with CO₂ gas for 1 hour. When the desired temperature (5 °C or 30 °C) of the electrolyte was attained, the pH of the test solution was adjusted from the equilibrium pH to the desired pH 5 by adding a deoxygenated sodium bicarbonate (NaHCO₃) solution. The working electrode, a carbon steel (X65) rotating cylinder previously polished by 600 grit silicon carbide paper, was inserted into the electrolyte as shown in *Figure 7*. The rotation speed of the working electrode was set at 1000 rpm. A potentiostat was connected to the three-electrode glass cell and the open circuit potential is monitored. The electrochemical measurements were carried out when a stable potential was established, after 5 to 30 minutes. The procedure

described above is the initial step and common for all the corrosion inhibition tests performed in the glass cells.

2.3.1 Corrosion inhibition above the wax appearance temperature (WAT)

Three steps, which include partitioning, corrosion inhibition and persistency, were performed for tests at temperature above the WAT (30 °C). These steps start with the initial steps listed in the heading immediately above. It should be noted that for the “above WAT” tests, the temperature of electrolyte is adjusted to 30 °C in the initial step and kept at 30 °C for all of the remaining steps.

Step 1: Partitioning

The partitioning step is employed to show whether Eicosane has a tendency to partition into the water phase from the oil phase and how it affects the corrosion rate when the temperature is above the WAT. In this step 0.25 L of synthetic paraffin-oil mixture at the same temperature (30 °C) as the electrolyte was added slowly on the top of the water phase. Because of the lower density of the oil, the oil mixture will float on top of the water. Thus, the carbon steel rotating cylinder is always immersed in water. The open circuit potential was carried out until a stable potential is established. Corrosion rate was measured every 20 minutes for 3-6 hours.

Step 2: Corrosion inhibition

The corrosion inhibition step follows the previous Partitioning step. The corrosion inhibition step is done to verify whether the layer of the synthetic paraffin-oil mixture

which coats the work electrode surface can affect the corrosion rate when the temperature is above the WAT. In this step the working electrode was moved up into the oil phase, which floats on the water phase, and rotated there for 15 minutes. The aim of moving the working electrode up and keeping it in the oil mixture is to sufficiently expose the working electrode to the synthetic paraffin-oil mixture. Then the working electrode was placed back into the water phase and the corrosion rate was measured. This “up-and-down” process was repeated every 20 minutes for 4 to 7 hours.

Step 3: Persistency

When the corrosion inhibition step is completed, the next step is to measure the persistency of any effect observed in the previous Corrosion Inhibition Step 2. After the last repeated cycle done in Step 2, the working electrode was kept steadily in the water phase. Corrosion rate measurements were conducted every 20 minutes for another 6 to 10 hours.

2.3.2 Corrosion inhibition below the wax appearance temperature (WAT)

All of the following tests were initiated the same way as the series of tests described above out, however, the temperature of the electrolyte was adjusted to 5 °C and kept at that temperature during the whole measurement. Two of the steps described above including the partitioning and the corrosion inhibition and persistency were employed in a similar fashion to test the corrosion behavior at temperature below the WAT (5 °C).

Step 1: Partitioning

In this test 0.25 L of the synthetic paraffin-oil mixture liquid which is slightly above the WAT was added slowly on the top of the water phase and the temperature of both water phase and oil phase was adjusted to 5 °C again. Because the temperature was lower than the WAT, the oil phase floating on top of the water phase became solid, but the carbon steel rotating cylinder was still below surrounded by the aqueous electrolyte. The open circuit potential was carried out until a stable potential was established. Corrosion rate was measured every 20 minutes for 3-6 hours. This step is employed to show whether Eicosane has a tendency to partition into water phase from oil phase and how it affects the corrosion rate when the temperature is below the WAT.

Step 2: Corrosion inhibition and persistency

This combined corrosion inhibition and persistency step immediately follows by the partitioning step. Because the synthetic paraffin-oil mixture is solid below the WAT, the corrosion inhibition cannot be measured by the same procedure as is shown in Section 2.3.1 for the “above the WAT” measurements. Thus, a different procedure was established.

Procedure 1:

The working electrode was prepared according to the initial step and immersed in synthetic paraffin-oil mixture at a temperature slightly above the WAT (1 °C higher than the WAT of each synthetic paraffin-oil mixture) for 15 minutes. It was then extracted

from the synthetic paraffin-oil mixture and cooled at 5 °C for 5 minutes until a wax layer appeared on the carbon steel surface visibly by the naked eye. Meanwhile, a glass cell was prepared following the same procedure as described above for the initial step. The glass cell temperature was adjusted to 5 °C. Then the freshly prepared working electrode was inserted into the water phase of the glass cell to measure the corrosion rate every 20 minutes for 10 hours. The aim of this step is to test whether the layer of the synthetic paraffin-oil mixture, which coats the working electrode, can significantly reduce the corrosion rate when the temperature is below the WAT, and if so, whether the corrosion inhibition is persistent.

However by using this procedure the specimen temperature quickly reaches the same temperature as the synthetic paraffin-oil mixture and is not well controlled, neither is the amount of wax that forms. Thus, a slightly different procedure was established as follows.

Procedure 2:

At the beginning, the working electrode was cooled to 5 °C and the synthetic paraffin-oil mixture was heated to the desired temperature (20 °C, 30 °C or 40 °C according to the test matrix in Table 3). After the temperature remained stable, the cooled working electrode was immersed in the heated oil mixture and quickly (within 1 second) removed from it. Due to the temperature difference, a wax layer formed on the surface. Next, the working electrode was inserted into the water phase in the glass cell at 5 °C and the corrosion rate was measured every 20 minutes at 1000rpm for 20-24 hours.

2.3.3 Effect of shear on corrosion inhibition

The aim of this test is to see if the wax layer on the specimen surface can be physically removed by shear stress. After preparing the working electrode according to the Procedure 1 and the Procedure 2 in the Step 2 of Section 2.3.2, the specimen with a wax layer was inserted into the water phase in the glass cell at 5 °C and the corrosion rate was measured every 20 minutes at 1000 rpm (linear velocity at specimen surface = 0.6 m/s) for 4-6 hours. After the corrosion rate became stable, the rotating speed was temporarily increased up to 9000 rpm (linear velocity at specimen surface = 5.6 m/s) for 1 hour. Then the rotation speed was slowed down to 1000 rpm again and the corrosion rate was measured. It should be noted that when rotation speed was 9000 rpm, no corrosion rate was measured. This procedure was repeated until the corrosion rate stops changing following the increase in the rotation speed.

2.3.4 Corrosion inhibition at a varying temperature

The aim of this series of tests was to see if the paraffin wax layer on steel surface can be removed by increasing temperature. If so, the mechanism of wax precipitating on steel surface would have been physi-sorption. The working electrode was immersed in the synthetic paraffin-oil mixture at a temperature slightly above the WAT (1 °C higher than the WAT of each synthetic paraffin-oil mixture) for 15 minutes, then moved out and cooled at 5 °C until a wax layer appeared and was clearly visible. Next, the specimen was inserted into the water phase in the glass cell at 5 °C and the corrosion rate was measured every 10 minutes at 5 °C for half an hour. Then the temperature was increased in 5 °C

increments up to 30 °C. The rotation speed of working electrode was kept at 1000 rpm. At each temperature, the corrosion rate was measured every 10 minutes for half an hour.

2.4 Wettability

One of the objectives of this project was to investigate the effect of paraffins on steel wettability, which was performed by measuring the contact angle of an oil droplet on a steel surface, surrounded by a water phase (oil-in-water scenario) or a water droplet in oil phase (water-in-oil scenario) at temperatures both above the WAT and below the WAT. *Figure 8(a)* shows the contact angle, θ , of a water droplet which is placed on the steel surface surrounded by an oil phase. *Figure 8(b)* shows the contact angle, θ , of an oil droplet which is placed beneath the steel surface surrounded by the water phase. The contact angle is defined as the angle between the surfaces of the droplet and the solid substrate line in contact with the water phase. A goniometer (*Figure 9*) is an instrument used for contact angle measurement. The goniometer is composed of two main parts: the test cell and the image capturing system. *Figure 10* shows the test cell of the goniometer with a carbon steel (X65) specimen on the specimen holder. Video of the oil (water) droplet is taken with an IMAGING PLANET[®] model 221-XS monochrome CCD video camera and the contact the angle of the oil/water droplet was measured using an image analysis software (the RINCON[®]). If the contact angle was larger than 90 °, the steel surface was deemed hydrophobic, otherwise, it was hydrophilic.

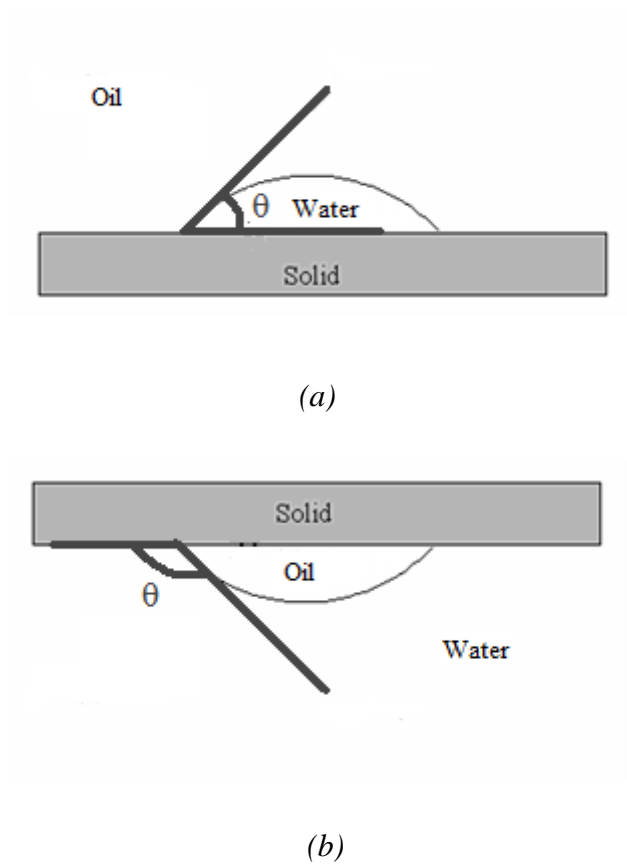


Figure 8. Sketch of the contact angle, θ , of (a) water droplet (water-in-oil) (b) oil droplet (oil-in-water).

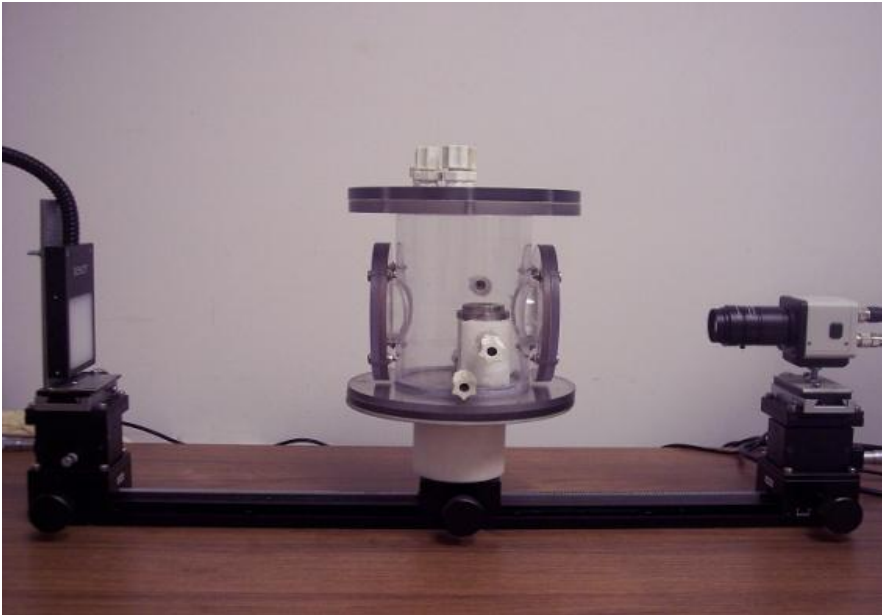


Figure 9. Goniometer setup with the video camera and a backlight. (courtesy of Xuanping Tang).

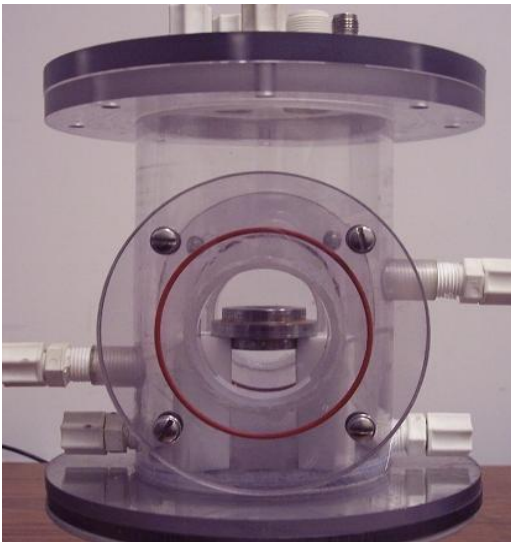


Figure 10. Test cell of goniometer with a carbon steel (X65) specimen on the specimen holder. (courtesy of Xuanping Tang).

Table 6 shows the test matrix for the contact angle measurements. Four different sets of wettability measurements were conducted as shown in Table 7.

Table 6. *Test Matrix for Contact Angle Measurement*

Parameter	Conditions
Oil phase	Synthetic paraffin-oil mixture
Water phase	CO ₂ saturated, 1 wt% NaCl aqueous solution, pH5
Temperature	5 °C (below the WAT), 30 °C (above the WAT)

Table 7. *Four Sets of Experiments for Wettability Measurement*

Set	Conditions
1	Oil droplet in water phase
2	Oil droplet in water phase (oil pre-wet specimen)
3	Water droplet in oil phase
4	Water droplet in oil phase (oil pre-wet specimen)

The differences between Set 1 and Set 2, Set 3 and Set 4 are explained in the following description of the procedures.

The detailed procedures for Set 1 and Set 3 are as follows.

1. Clean the test cell with soap, tap water followed by deionized water.
2. Put either 1 wt% NaCl aqueous solution or synthetic paraffin-oil mixture into the test cell until the liquid level is 3 cm higher than the specimen holder.
3. Purge the test cell with CO₂ for one hour.

4. Put the polished carbon steel specimen on the specimen holder.
5. Inject the droplet (either oil or water) on the specimen through the injection port.
6. Capture the droplet image with the video camera.
7. Analyze the droplet image and measure the contact angle using image analysis software.

It should be noted that because the synthetic paraffin-oil mixture is solid below the WAT (5 °C), the contact angle measurements could not be conducted below WAT.

The detailed procedures for Set 2 and Set 4 are as follows.

1. Clean the test cell with soap, tap water followed by deionized water.
2. Put either 1 wt% NaCl aqueous solution or synthetic paraffin-oil mixture into the test cell until the liquid level is 3 cm higher than the specimen holder. (For the measurements at a temperature below the WAT the LVT200 was used instead of synthetic paraffin-oil mixture because the synthetic paraffin-oil mixture is solid.
3. Purge the test cell with CO₂ for one hour.
4. Purge a 50 ml beaker which contains synthetic paraffin-oil mixture at a temperature slightly (1 °C) above the WAT with CO₂ for one hour.
5. Put the polished carbon steel specimen in the synthetic paraffin-oil mixture contained in the beaker for 15 minutes.
6. Move the specimen out and put it on the specimen holder. For the measurements at a temperature below the WAT, before putting it on the

specimen holder, keep the specimen at 5 °C for 5 minutes until a wax layer shows up visibly on the specimen surface.

7. Inject the droplet (either oil or water) on the specimen through the injection port. For the measurements at a temperature below the WAT, the LVT200 was used instead of synthetic paraffin-oil mixture because the synthetic paraffin-oil mixture is solid below the WAT.
8. Capture the droplet image with the video camera.
9. Analyze the droplet image and measure the contact angle using the image analysis software.

2.5 Interfacial tension

A tensiometer (*Figure 11*) manufactured by the CSC Scientific Company (model NO. 70545) uses a platinum ring to measure the oil and water interfacial tension. The principle of the tensiometer is that when the withdrawal force (upward) exerted externally on the platinum ring is larger than the force (downward) caused by interfacial tension between oil and water, the film at the interface on the platinum ring breaks. In this research, the platinum ring was pulled upwards from water phase toward the oil phase at the oil water interface. The detailed procedure is shown below. The interfacial tension is measured in dyne per centimeter (dyne/cm), which is equivalent to milliNewtons per meter (mN/m).



Figure 11. Setup of tensiometer using a platinum ring to measure the interfacial tension between water and oil.

Table 8 shows the test matrix for the interfacial tension measurements.

Table 8. Test Matrix for Interfacial Tension Measurements

Parameter	Conditions
Oil phase	Synthetic paraffin-oil mixture
Water phase	CO ₂ saturated, 1 wt% NaCl aqueous solution, pH=5
Temperature	30 °C (above the WAT)

The detailed procedure for this measurement is described as follows.

1. Clean the sample glass container with soap, tap water followed by deionized water.
2. Add 1 wt% NaCl aqueous solution at 30 °C into the sample glass container to a depth of 10 -15 mm.
3. Place the container on the sample table, which is raised until the platinum ring is immersed 5-7 mm in the water.
4. Pipette the synthetic paraffin-oil mixture oil at 30 °C on the top of the water phase until a depth is 10 mm.
5. Lower the position of the sample table and adjust the knurled knob simultaneously to maintain the ring in the interface and the torsion arm in the zero position of the index.
6. When the liquid film at the interface on the platinum ring ruptures, the reading on the dial is the oil and water interfacial tension in dyne/cm.
7. Repeat this experiment 3-5 times and determine the mean and the standard deviation.

CHAPTER 3: RESULTS AND DISCUSSION

The experimental results for the properties of the synthetic paraffin-oil mixture properties, wax precipitation on the steel surface and the small scale experiments including corrosion inhibition, wettability (contact angle) and interfacial tension are presented in this chapter. The test matrices, experimental setup and procedures are described in Chapter 2. The thermodynamic model of wax precipitation will be introduced in Chapter 4.

3.1 Properties of the synthetic paraffin-oil mixture

The following physical properties of the synthetic paraffin-oil mixture were measured: viscosity, wax appearance temperature (WAT) and density. The test matrix for these measurements is shown in Table 2 (page 26).

3.1.1 Viscosity

The viscosity is tested by a Haake viscometer described in Chapter 2 at room temperature. The procedure for the viscosity measurement is described in Section 2.1.1. *Figure 12* shows the viscosity of synthetic paraffin-oil mixture at different concentrations of Eicosane at room temperature. The aim of testing the viscosity of the synthetic paraffin-oil mixture was to establish whether it is similar to the crude oil. It can be seen that the more Eicosane is added, the higher the viscosity becomes. The addition of 10, 30 and 50 wt% Eicosane increases the viscosity of LVT200 by 12%, 29% and 47%, respectively. Although the addition of Eicosane increases the viscosity significantly, compared to the heavy crude oil which has a viscosity of more than 10,000 cP, the

synthetic paraffin-oil mixtures for this research are much less viscous and similar to each other. Also, because the LVT200 is a highly refined oil which is used to produce gasoline, the viscosity of the synthetic paraffin-oil mixture is similar to the highly refined oil. Therefore, it can still be employed to isolate the effect of paraffins and make the paraffins easier to investigate.

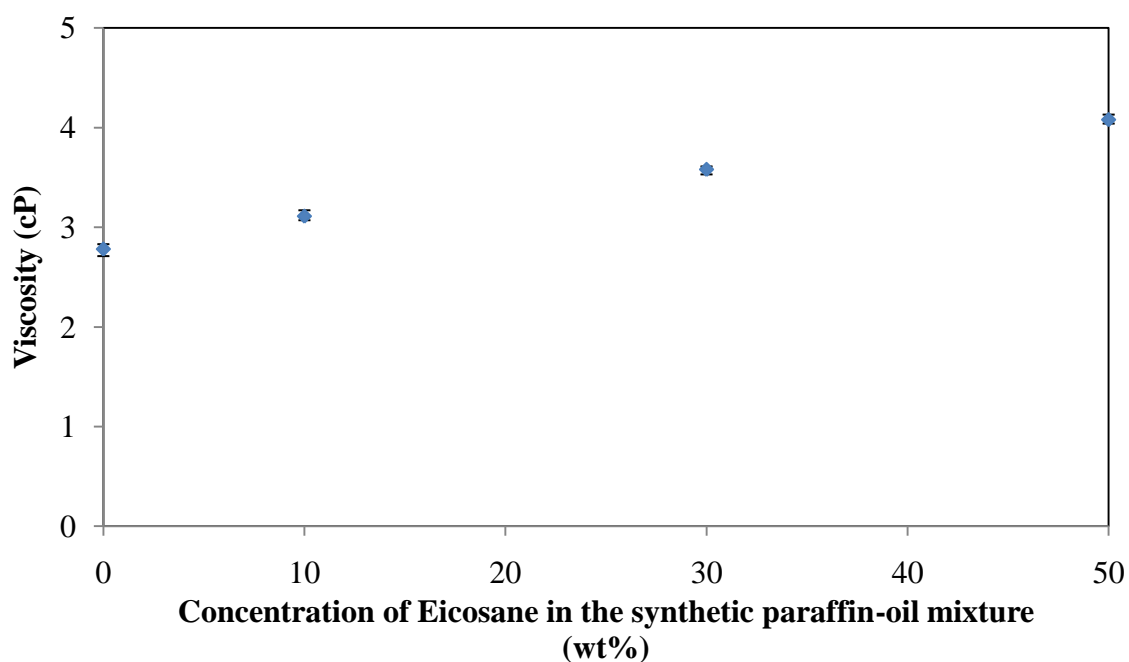


Figure 12. Viscosity of the synthetic paraffin-oil mixture at room temperature.

3.1.2 Wax appearance temperature (WAT)

The wax appearance temperature (WAT) is tested using an apparatus including an ice bath and a thermocouple. The procedure for the WAT measurements is described in Section 2.1.2. Figure 13 shows the WAT of the synthetic paraffin-oil mixture at different concentrations of Eicosane. As seen from the Figure, the WAT increases from 7 °C (10

wt% Eicosane) to 35 °C (100 wt% Eicosane) as the concentration of Eicosane increases. The WAT was measured to choose the appropriate temperature for conducting the measurements throughout this research program. Therefore, the temperature of 5 °C was chosen as the temperature below the WAT and 30 °C as the temperature above the WAT for all measurements independent of the Eicosane concentrations because 10, 30 and 50 wt% synthetic paraffin-oil mixtures were used.

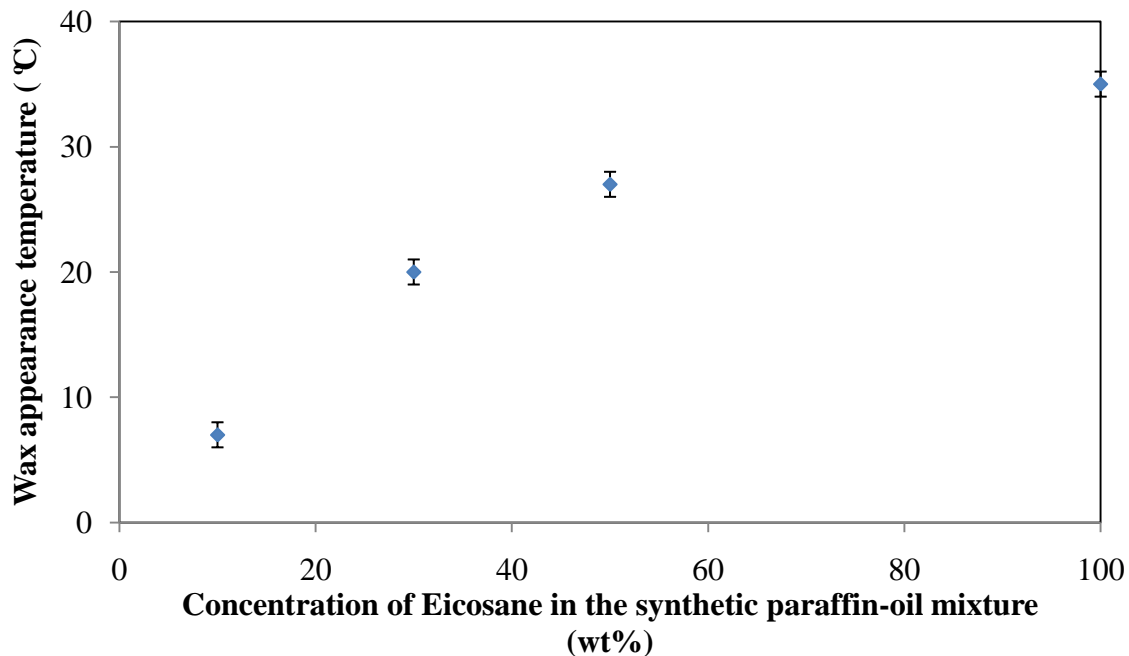


Figure 13. Wax appearance temperature (WAT) of the synthetic paraffin-oil mixture.

3.1.3 Density

The density of synthetic paraffin-oil mixture is measured using a balance and a 100 ml graduated cylinder at room temperature. The procedure for this measurement is described in Section 2.1.3. *Figure 14* is the density of the synthetic paraffin-oil mixture at

different concentrations of Eicosane. It can be seen that with the addition of Eicosane, the density of synthetic paraffin-oil mixture decreases from 0.825 g/cm^3 (LVT200) to 0.805 g/cm^3 (50 wt% Eicosane). This agrees with the fact that the density of the Eicosane (0.79 g/cm^3 at room temperature) is lower than that of LVT200. Generally, the light crude oil has a density lower than 0.83 g/cm^3 , thus, with the highest density of 0.825 g/cm^3 , the synthetic paraffin-oil mixture can be classified as light oil.

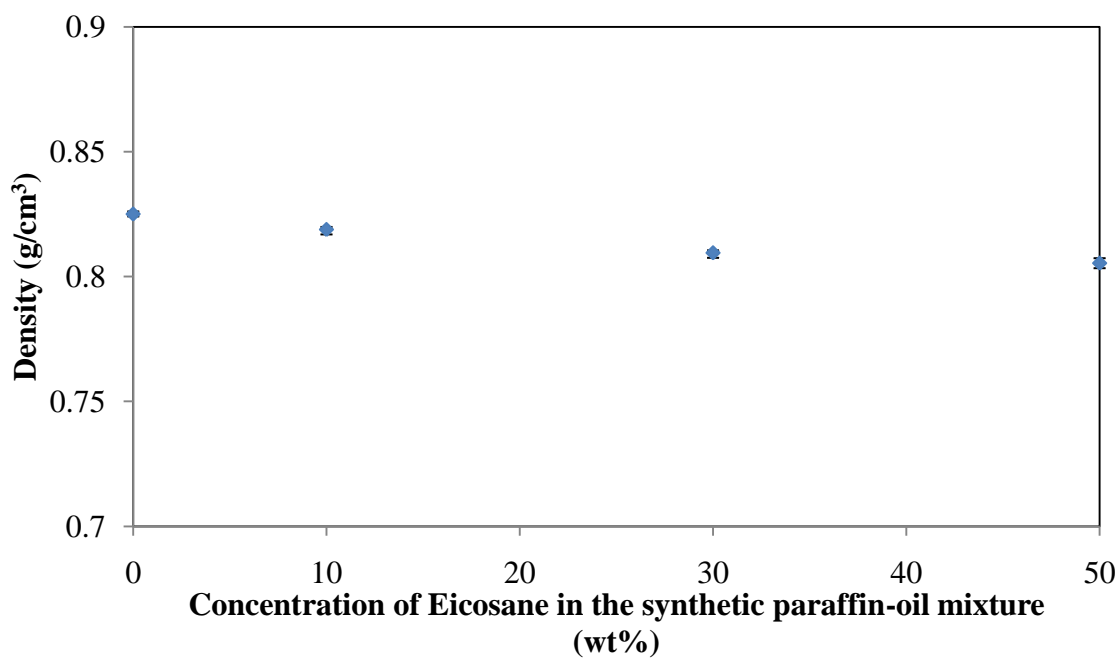


Figure 14. Density of the synthetic paraffin-oil mixture at room temperature.

3.2 Wax precipitation on the steel surface

The detailed information including test matrix, experimental setup and procedure can be found in Section 2.2. Synthetic paraffin-oil mixture with concentration of 30 wt% Eicosane is selected as the wax source. Three oil temperatures are chosen: 20, 30 and

40 °C. The specimen temperature is set at 5 °C. Hence the temperature differences between the specimen and oil are 15, 25 and 35 °C, respectively. *Figure 15* shows the weight of the wax precipitation as a function of time and oil temperature.

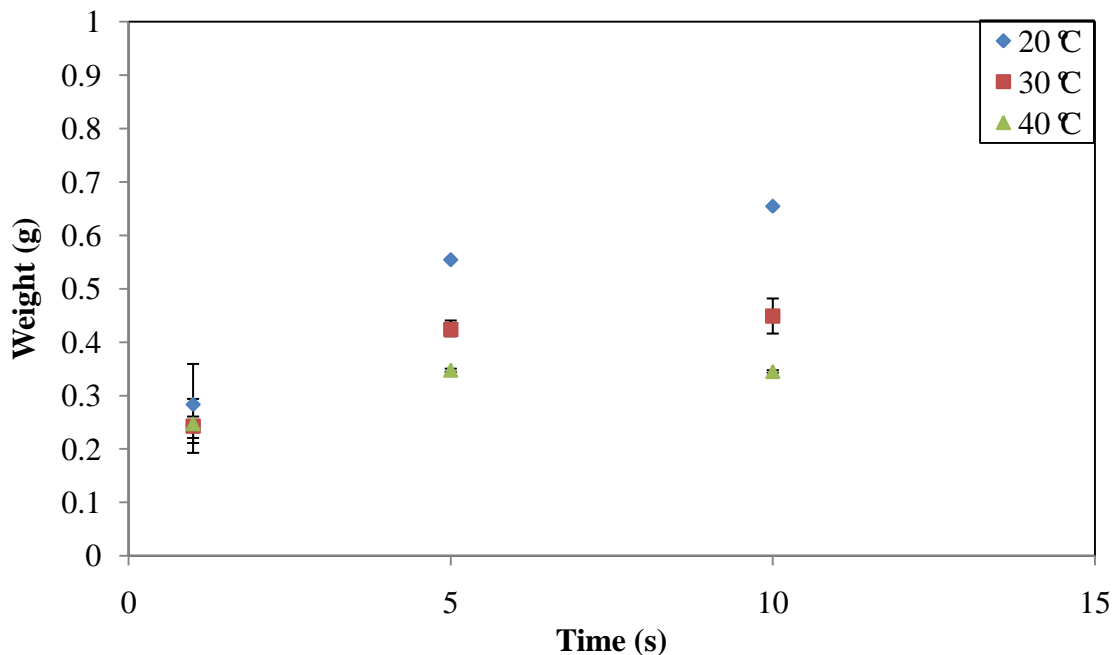


Figure 15. Weight of wax precipitation as a function of time and oil temperature. Wax source: 30 wt% synthetic paraffin-oil mixture. Specimen temperature: 5 °C.

As seen from *Figure 15*, the weight of the wax precipitation increases with time and decreases with temperature difference. At 1 second exposure, the weight of the wax precipitation is nearly the same (0.25 g) for the three oil temperatures. For longer exposure time, the difference among wax weights for the three oil temperatures increases. At 10 second exposure, the difference of weight of wax between oil at 20 °C and 40 °C is 0.3 g. Also, we can conclude from the Figure, the weight of wax for 20 °C is continuously

increasing, while for 40 °C it is stable. Therefore, the wax weight in these experiments was proportional to time and inversely proportional to oil temperature.

3.3 Corrosion inhibition

This section is divided into 4 parts: corrosion inhibition above the WAT, corrosion inhibition below the WAT, effect of shear on corrosion inhibition, corrosion inhibition at varying temperature. The test matrix for the corrosion inhibition measurements is shown in Table 3 (page 32).

3.3.1 Corrosion inhibition above the wax appearance temperature (WAT)

The procedure for this measurement is described in Section 2.3.1 in Chapter 2. *Figure 16* shows the plot of corrosion rate (mm/yr) vs. time (hr) for different concentration of the synthetic paraffin-oil mixture during the three steps: partitioning, corrosion inhibition and persistency, when the temperature is above the WAT (30 °C) using the LPR technique. LPR technique is explained in APPENDIX A.

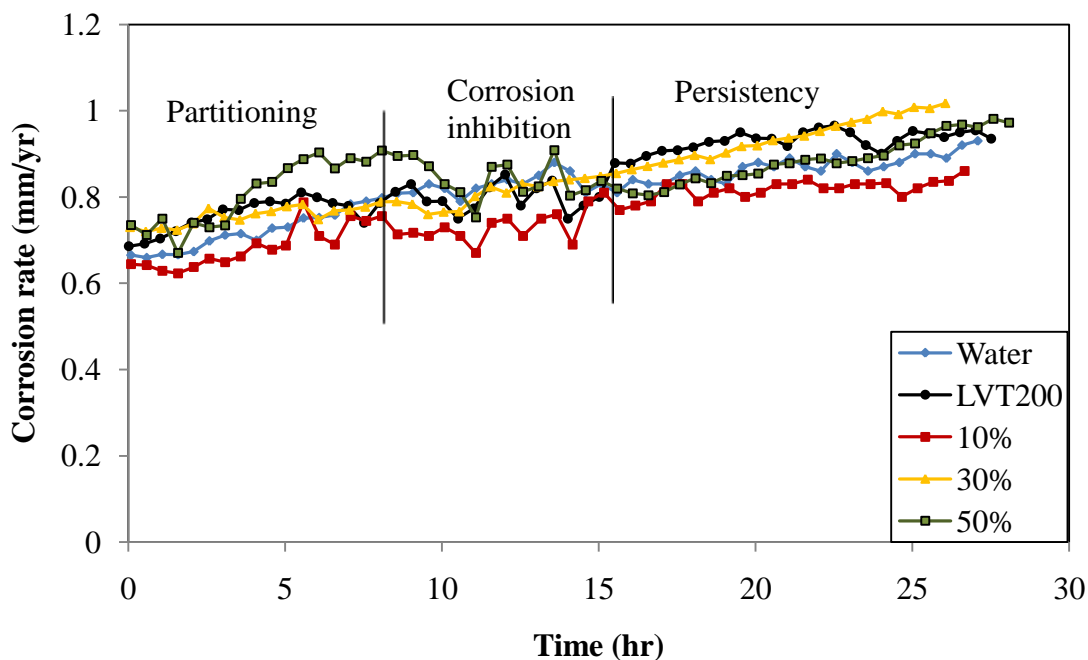


Figure 16. LPR results of 3 steps of corrosion inhibition measurement for the synthetic paraffin-oil mixture at 30 °C (above the WAT).

The partitioning step in *Figure 16* shows that there is no significant difference in the corrosion rate among different synthetic paraffin-oil mixtures and baseline, indicating that paraffins (Eicosane) do not partition into the water phase from oil phase and therefore do not affect the corrosion rate of the steel surface this way. Because paraffins are water insoluble, it is not expected that partitioning will occur.

It can be seen from the corrosion inhibition step seen in *Figure 16* that the corrosion rates for different synthetic paraffin-oil mixtures are nearly the same as the baseline within the error of measurement. This means when the temperature is above the wax appearance temperature, paraffins (Eicosane) do not generate corrosion inhibition,

which indicates that there is no adsorption on the specimen surface. This is due to the non-polar nature of the paraffins.

In the persistency step, when the temperature was above the wax appearance temperature, no change in the corrosion rate was observed as compared to the first two steps. The corrosion rate continues to be the same, which is because there is no adsorption or deposition on the specimen surface since no protective layer is formed.

3.3.2 Corrosion inhibition below the wax appearance temperature (WAT)

Two steps are conducted when performing tests at a temperature below the WAT (5 °C). The procedure of this measurement is described in Section 2.3.2.

Step 1. Partitioning

Figure 17 shows the LPR results of the corrosion rate (mm/yr) vs. time (hr) at different concentration of paraffins during the partitioning step at 5 °C. As seen from *Figure 17*, the steady state corrosion rate for the baseline with pure water is 0.25 mm/yr at 30 °C. The corrosion rates for all the synthetic paraffin-oil mixtures are the same as the baselines, which indicates that paraffins (Eicosane) do not partition into the water phase from the oil phase and therefore do not affect corrosion rate when the temperature is below the WAT.

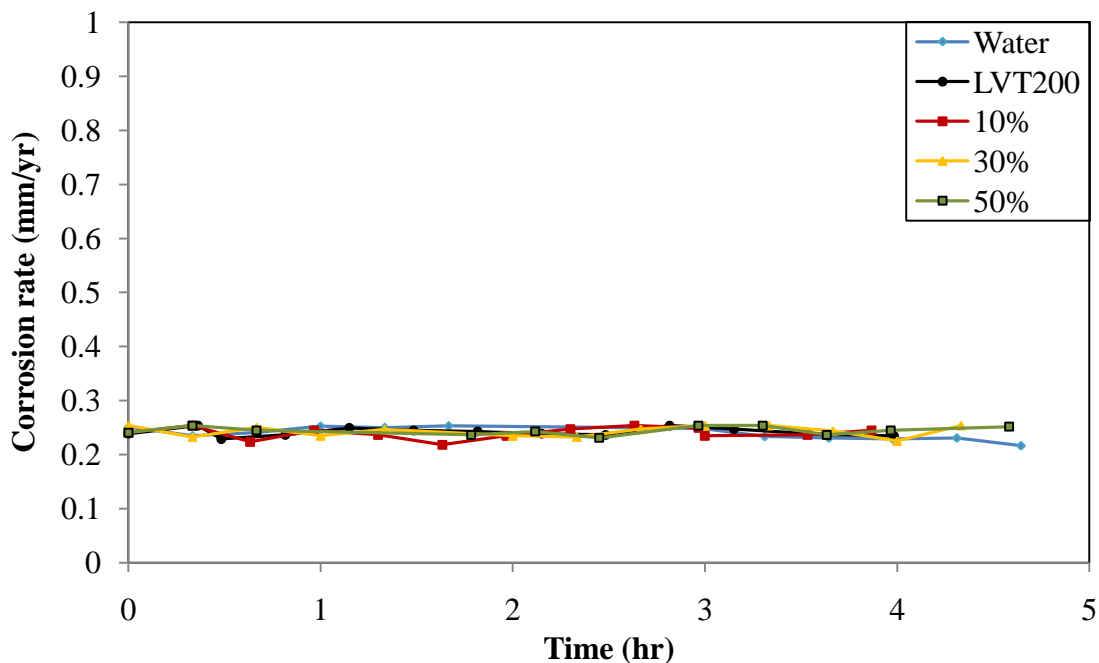


Figure 17. LPR results of the partitioning step for the synthetic paraffin-oil mixture at 5 °C (below the WAT).

Step 2. Corrosion inhibition and persistency

Two different procedures are conducted for Step 2. The results for these two procedures are shown below.

Procedure 1:

Figure 18 shows the LPR results of corrosion rate (mm/yr) vs. time (hr) at different concentration of paraffins during the corrosion inhibition and persistency step. Compared to the corrosion rates for water and LVT200 baselines, it can be seen that the corrosion inhibition generated by the synthetic paraffin-oil mixtures at the higher concentrations of Eicosane (30 wt% and 50 wt%) is larger than the lower one (10 wt%).

The corrosion inhibition generated by 30 wt% and 50 wt% synthetic paraffin-oil mixtures is nearly 90% compared to the baseline. This suggests that the corrosion rate is reduced with the addition of paraffins (Eicosane), which means that paraffins produce significant corrosion inhibition at temperatures below the WAT. *Figure 18* also suggests that this corrosion inhibition is persistent with time.

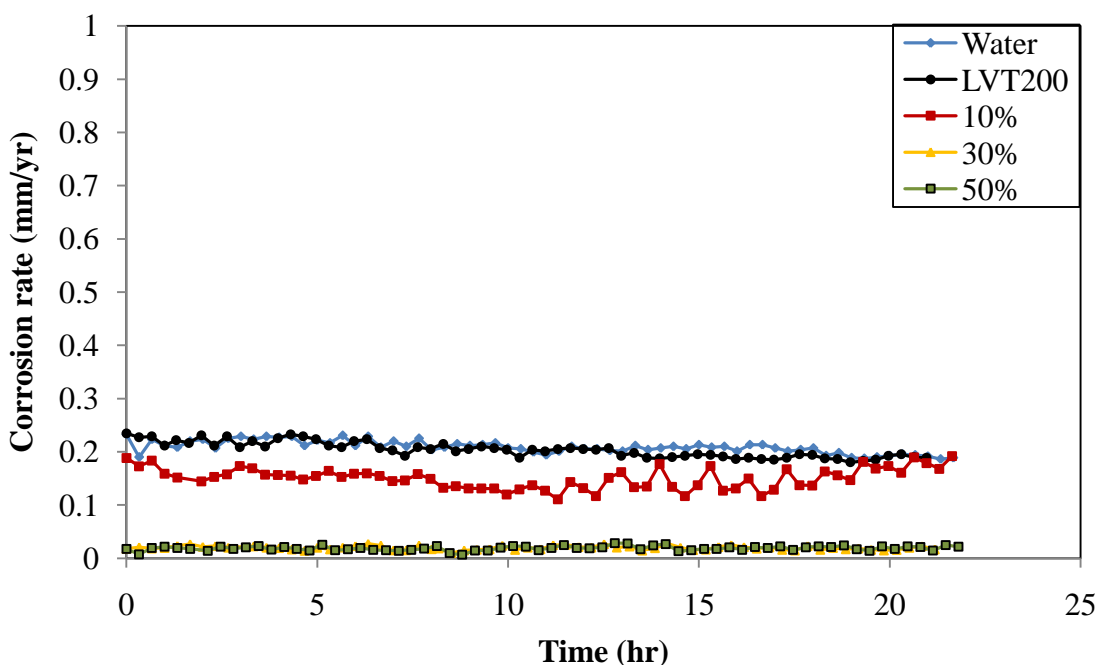


Figure 18. LPR results of the corrosion inhibition and persistency step for Procedure 1 at 5 °C (below the WAT).

Procedure 2:

The corrosion inhibition measurement for this procedure is done using 30 wt% hot synthetic paraffin-oil mixture with 1 second immersion of a cold working electrode which is at 5 °C and then quickly removed from it.

Figure 19 shows the LPR results of corrosion rate (mm/yr) vs. time (hr) at different oil temperature (20, 30 or 40 °C), while the specimen temperature is set at 5 °C. It can be seen that the steady state corrosion rate for the water baseline is 0.25 mm/yr. The corrosion inhibition generated by 30 wt% synthetic paraffin-oil mixture at three different oil temperature is the same. The wax formation at these three temperatures all generates 90% corrosion inhibition, the same as what 30 wt% synthetic paraffin-oil mixture did in *Figure 18*. This suggests that wax formation due to temperature difference at condition of 1 second can produce significant corrosion inhibition at temperatures below the WAT. *Figure 19* also suggests that this corrosion inhibition is persistent with time.

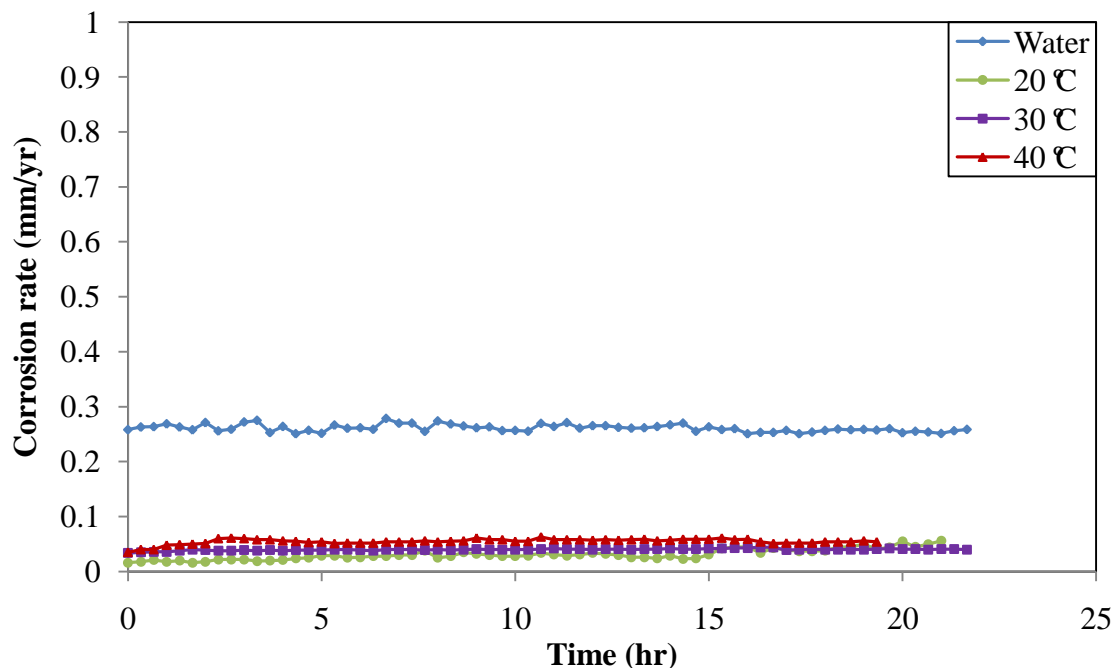


Figure 19. LPR results of the corrosion inhibition and persistency step for Procedure 2 at 5 °C (below the WAT). (Oil source: 30 wt% synthetic paraffin-oil mixture. Specimen temperature: 5 °C.)

3.3.3 Effect of shear on corrosion inhibition

The aim of this test is to see if the wax layer on the specimen surface can be physically removed by shear stress. The procedure is described in Section 2.3.3.

Figure 20 shows the LPR results of corrosion rate (mm/yr) vs. time (hr) for testing the effect of shear on corrosion inhibition. Synthetic paraffin-oil mixture with concentration of 30 wt% Eicosane is selected to conduct this experiment. The specimen preparation for this experiment is described in Procedure 1 of Part 2 of Section 2.3.2. All the points in *Figure 20* are obtained at 1000 rpm, while the arrows showing 9000 rpm indicate that rotation speed was increased to 9000 rpm for short periods of time in between the measurements which were all done at 1000 rpm (see the experimental procedure at page 41). From *Figure 20*, it can be seen that without increasing peripheral velocity, the 30 wt% synthetic paraffin-oil mixture generates 90% corrosion inhibition compared to the water baselines. After increasing the peripheral velocity (shear) of the rotating cylinder, the corrosion inhibition is reduced and the corrosion rate almost returns to the water baseline. This means that increasing the shear affects the corrosion rate by physically removing the wax layer on the steel surface.

Figure 21 shows the LPR results of corrosion rate (mm/yr) vs. time (hr) for testing the effect of shear on corrosion inhibition. The specimen preparation for this experiment is described in Procedure 2 of Part 2 of Section 3.3.2. The synthetic paraffin-oil mixture with concentration of 30 wt% Eicosane at three different temperatures (20, 30 and 40 °C) is selected to conduct this experiment. All the points in *Figure 21* are tested at 1000 rpm, while 9000 rpm was used in between the points (see the experimental

procedure at page 41). From *Figure 21*, it can be seen that without increasing peripheral velocity, all the 30 wt% synthetic paraffin-oil mixture at the three different temperatures generate 90% corrosion inhibition compared to the water baselines. After increasing the peripheral velocity (shear) of the rotating cylinder, the corrosion inhibition is reduced and the corrosion rate almost returns to the water baseline. This means that increasing the shear affects the corrosion rate by physically removing the wax layer on the steel surface.

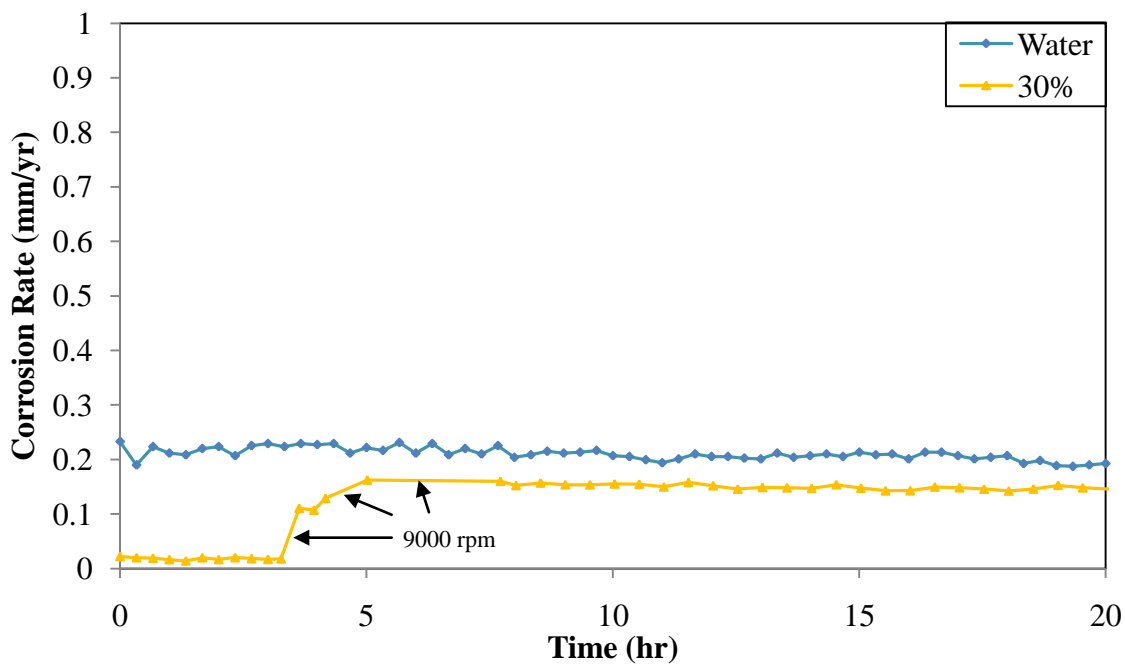


Figure 20. LPR results for testing the effect of shear on corrosion inhibition.

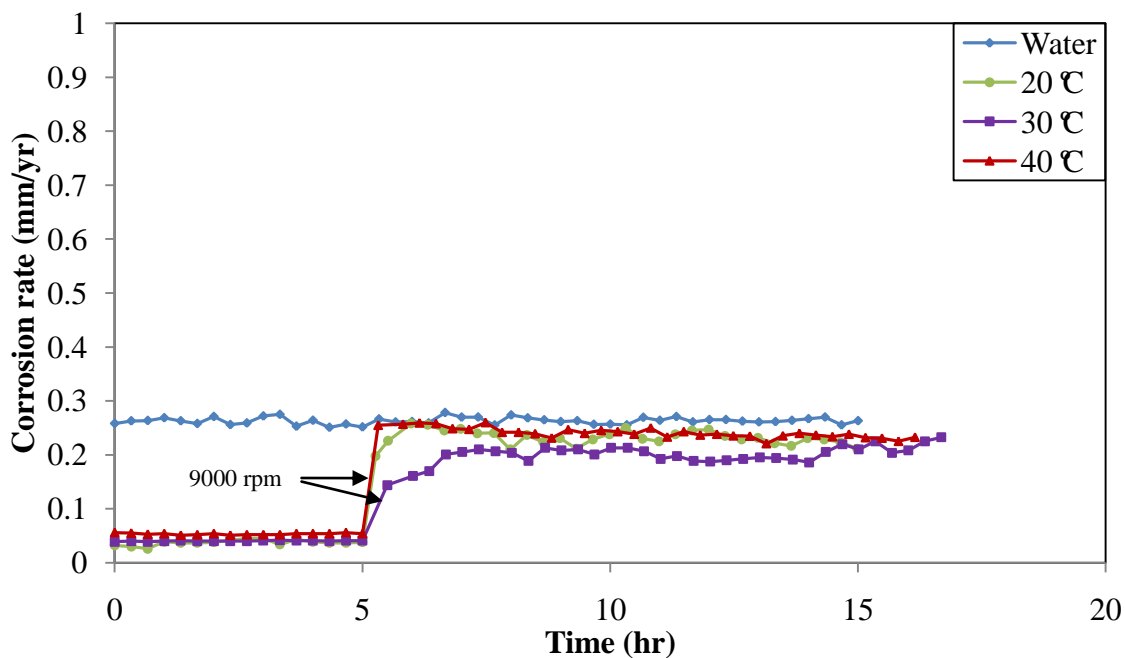


Figure 21. LPR results for testing the effect of shear on corrosion inhibition.

3.3.4 Corrosion inhibition at a varying temperature

The aim of this test is to see if the paraffin wax layer on steel surface can be physically removed by increasing temperature. *Figure 22* shows the LPR results for 6 temperatures from 5 °C to 30 °C in 5 °C increments (see the procedure for these measurements in Section 2.3.4 on page 41). The synthetic paraffin-oil with the concentration of 30 wt% Eicosane is selected to conduct this experiment. It can be seen that the corrosion rate returns to the original corrosion rate, as seen in *Figure 16* (page 56) for 30 wt% Eicosane, after the temperature was gradually increased from 5 °C to 30 °C, indicating that the mechanism of paraffin precipitation on steel surface is physisorption.

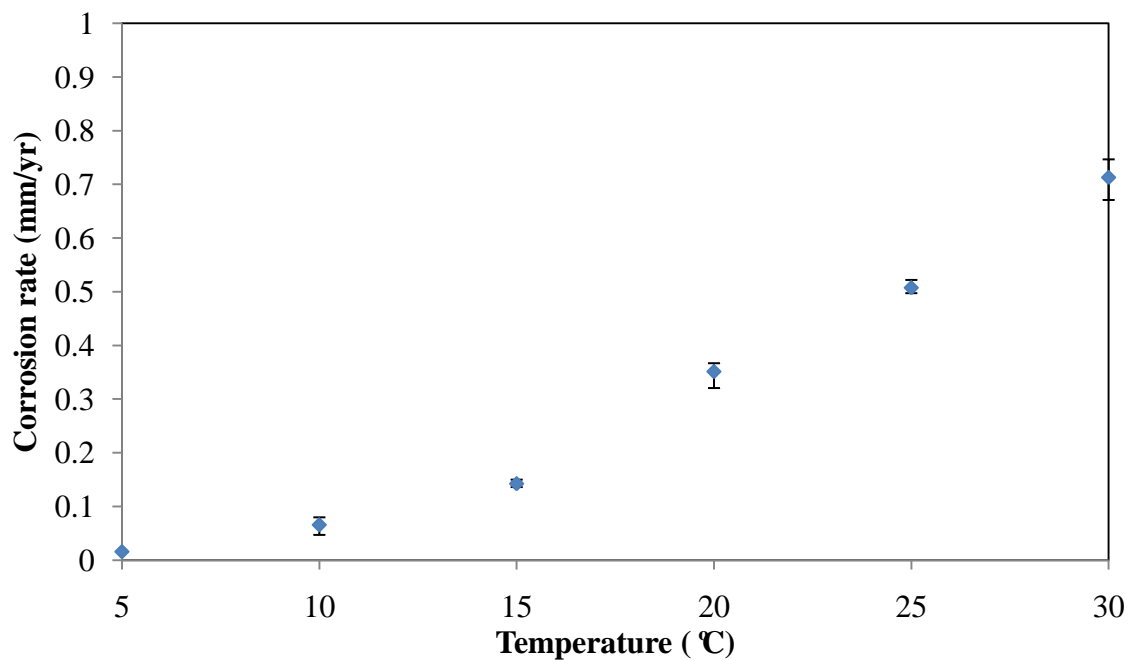


Figure 22. LPR results for testing the effect of increasing the temperature from 5 °C to 30 °C on corrosion inhibition.

3.4 Wettability

A goniometer is employed to conduct wettability measurements by measuring contact angle of an oil droplet on the steel surface, surrounded by water phase (oil-in-water) or a water droplet in oil phase (water-in-oil) at temperatures above the WAT and below the WAT. *Figure 8* (page 43) shows a sketch of how contact angles are determined. The procedure for contact angle measurements is described in Section 2.4, and Table 6 (page 45) shows the test matrix of contact angle measurements. Four different sets of wettability measurements are conducted shown in Table 7 (page 45).

3.4.1 Oil droplet in water phase

Figure 23 shows images of contact angle measurements for droplets of synthetic paraffin-oil mixture at different concentrations of Eicosane in 1 wt% NaCl aqueous solution (water) phase at 30 °C. Each image is labeled showing the composition of oil droplet and the contact angle it formed at the specimen surface.

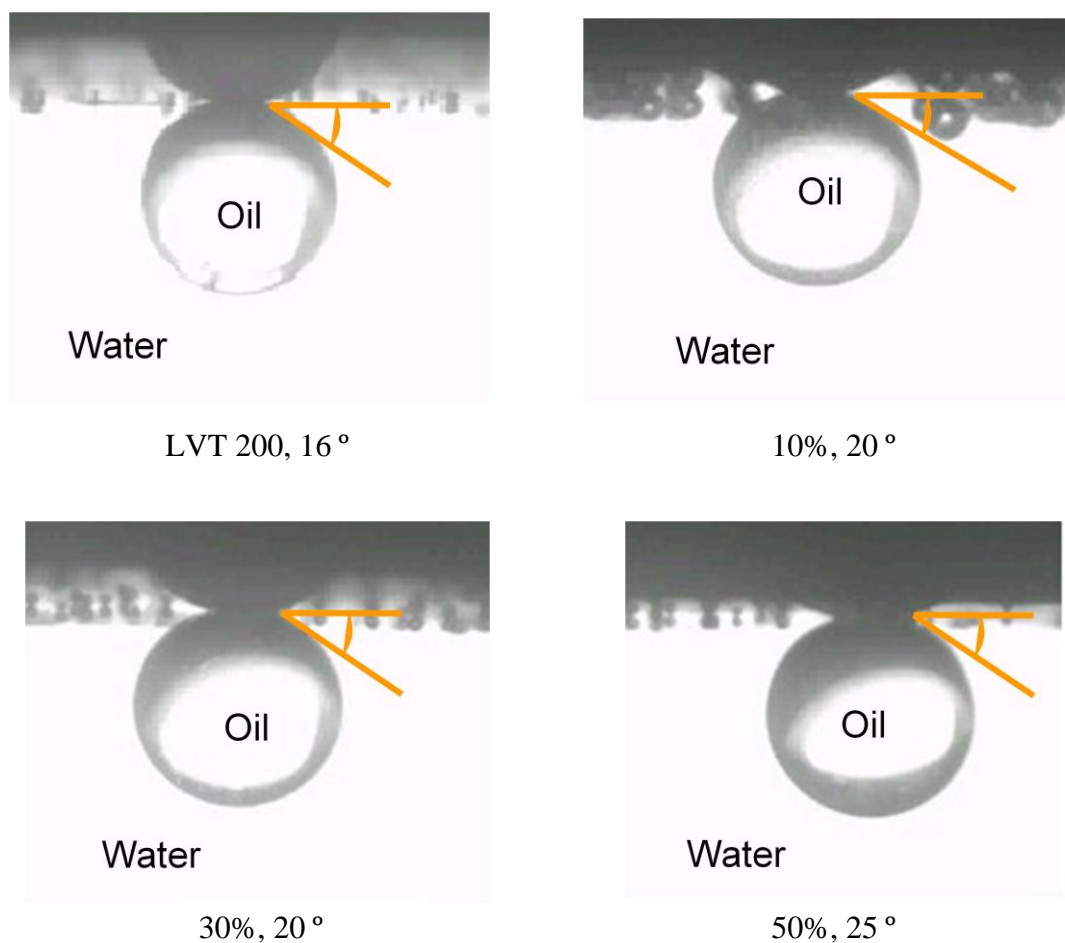
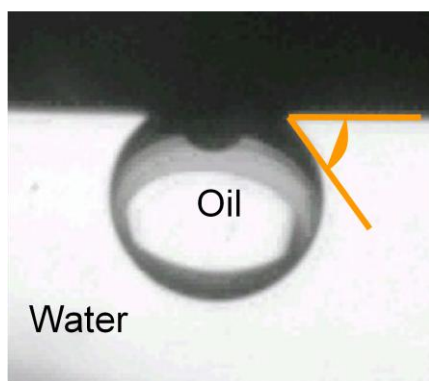


Figure 23. Droplets of the synthetic paraffin-oil mixture on the surface of the carbon steel (X65) in 1 wt% NaCl aqueous solution (water) phase at 30 °C.

Because the synthetic paraffin-oil mixture is solid below the WAT (5 °C), the contact angle measurements cannot be conducted. *Figure 24* only shows images of contact angle measurements for droplets of LVT 200 in 1 wt% NaCl aqueous solution (water) phase at 5 °C. Below the image, the composition of oil droplet (LVT200) and the contact angle it formed at the specimen surface is shown.



LVT 200, 37 °

Figure 24. Droplet of LVT200 on the surface of carbon steel (X65) in 1 wt% NaCl aqueous solution (water) phase at 5 °C.

Figure 25 shows the plot of contact angle measurements with synthetic paraffin-oil mixture droplets in 1 wt% NaCl aqueous solution (water) phase at 5 °C and 30 °C. From *Figure 25*, when the temperature is 30 °C (above the WAT), contact angles of synthetic paraffin-oil mixtures at 4 different concentrations of Eicosane are the same and close to 20 °. When the temperature is 5 °C (below the WAT), the LVT200 droplet is 37 °. The steel surface tends to be hydrophilic at 30 °C (above the WAT) as well as at 5 °C (below the WAT). This means that the contact angle does not change with the addition of

paraffins (Eicosane) when the temperature is 30 °C (above the WAT), which implies that the addition of paraffins should not affect the wettability of the steel surface, which continues to be hydrophilic.

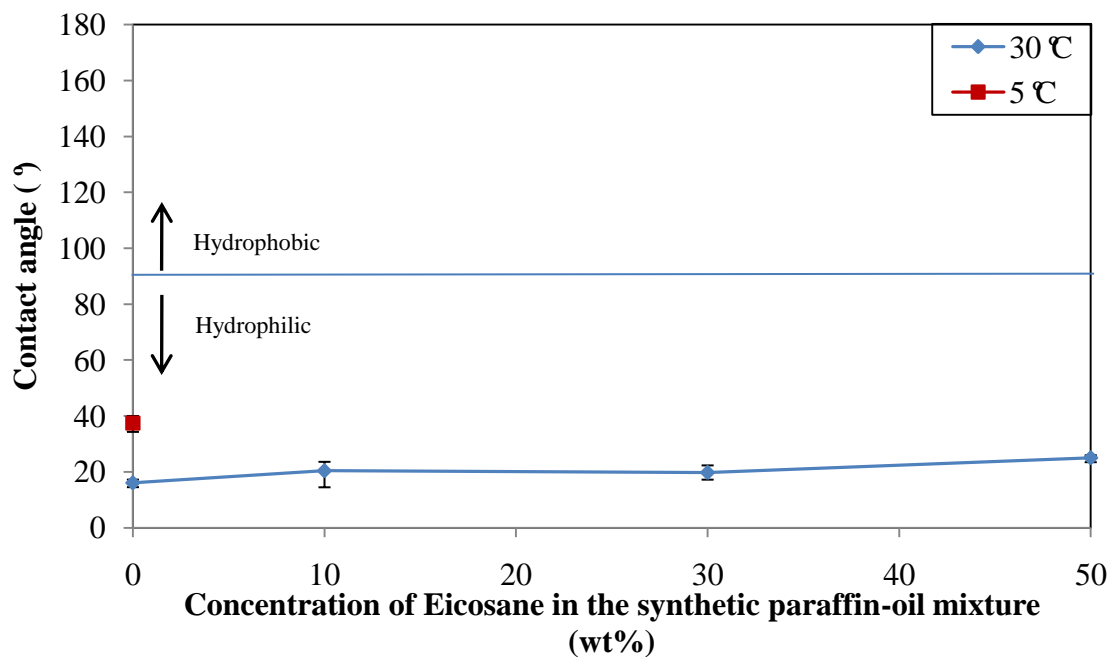


Figure 25. Contact angle measurements with droplets of the synthetic paraffin-oil mixture in 1 wt% NaCl aqueous solution (water) phase at 5 °C and 30 °C.

3.4.2 Oil droplet in water phase (oil pre-wet specimen)

Figure 26 shows images of contact angle measurements for LVT200 droplets in 1 wt% NaCl aqueous solution (water) phase at 30 °C (above the WAT) when the carbon steel (X65) specimen is pre-wetted by different concentrations of Eicosane in synthetic paraffin-oil mixture. Each image is labeled with the composition of the pre-wetted layer

on the specimen and the contact angle between the LVT200 droplet and the specimen surface.

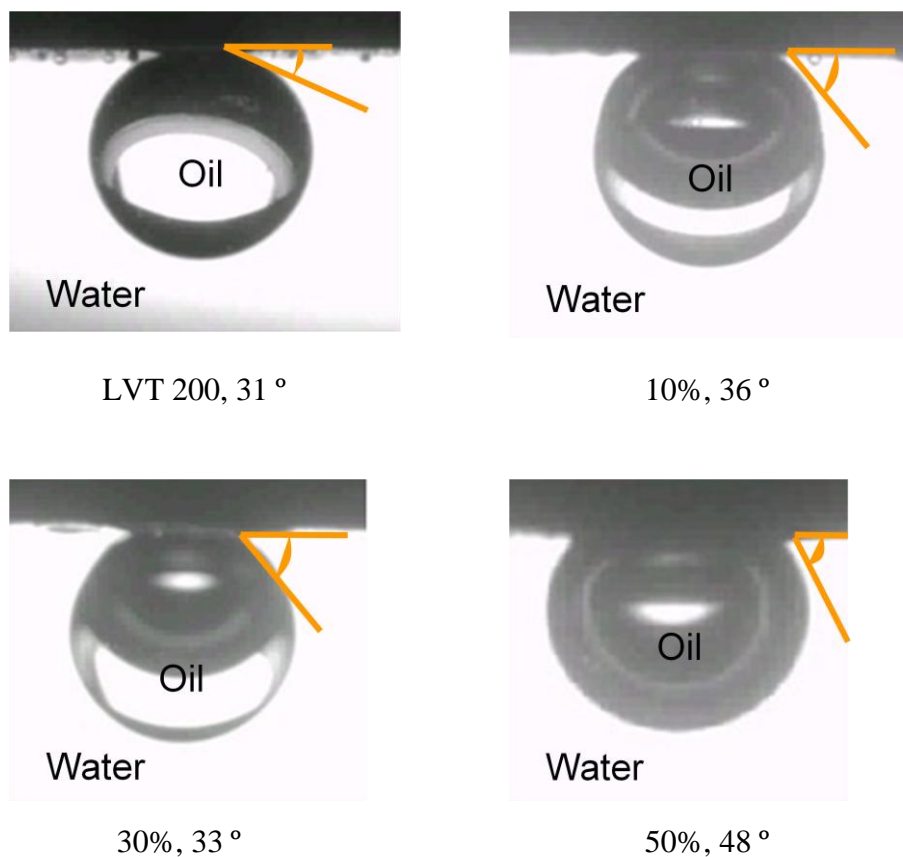


Figure 26. Droplets of the synthetic paraffin-oil mixture in 1 wt% NaCl aqueous solution (water) phase at 30 °C on the surface of carbon steel (X65) which is pre-wetted with the synthetic paraffin-oil mixture.

For the measurements at a temperature below the WAT (5 °C), the LVT200 droplet will be used instead of synthetic paraffin-oil mixture, because the synthetic paraffin-oil mixture is solid below the WAT.

Figure 27 shows images of contact angle measurements for LVT200 droplets in 1 wt% NaCl aqueous solution (water) phase at 5 °C (below the WAT), when the carbon

steel (X65) specimen is pre-wetted with different concentrations of Eicosane in synthetic paraffin-oil mixture. Each image is labeled with the composition of the pre-wetted layer on the specimen and the contact angle between the LVT200 droplet and the specimen surface.

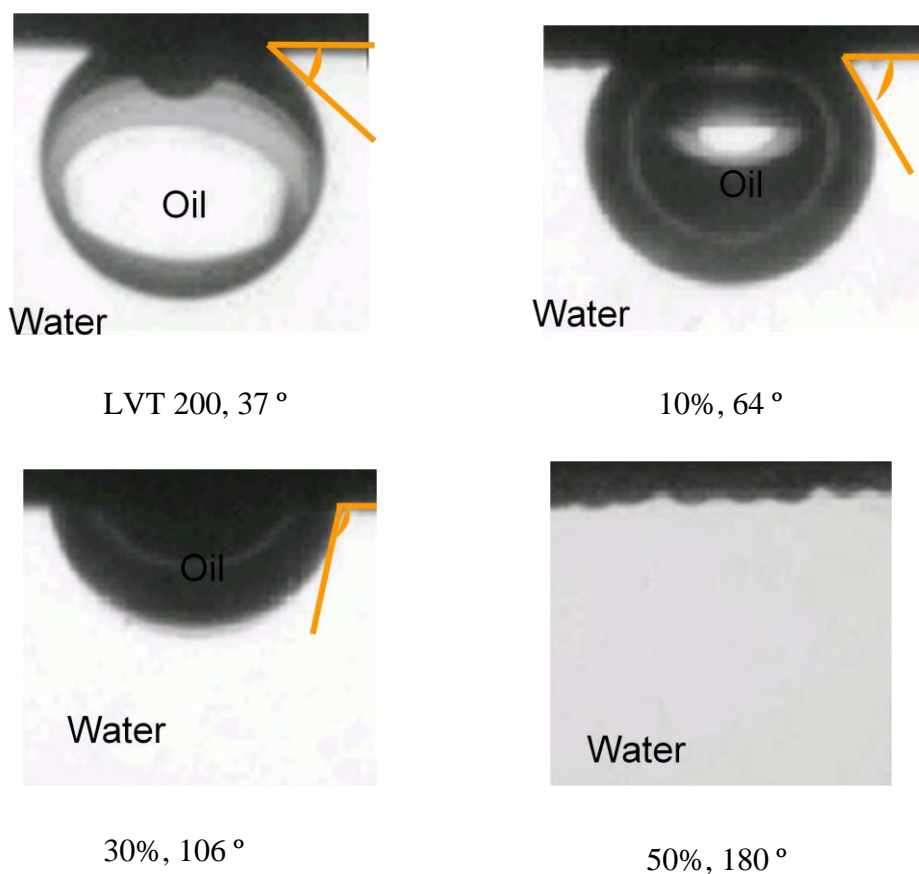


Figure 27. Droplets of LVT200 in 1 wt% NaCl aqueous solution (water) phase at 5 °C on the surface of carbon steel (X65) which is pre-wetted with the synthetic paraffin-oil mixture.

Figure 28 shows the plot of contact angle measurements of LVT200 oil droplets in 1 wt% NaCl aqueous solution (water) phase when the carbon steel (X65) specimen is pre-wetted with different concentrations of Eicosane in synthetic paraffin-oil mixture at

5 °C and 30 °C. Above the WAT, contact angles of synthetic paraffin-oil mixtures at 4 different concentrations of Eicosane are the same and close to 35 °, which means there is no significant change in the wettability of the steel surface, and it remains hydrophilic. When the temperature is below the WAT the contact angle changes significantly from 37 ° (LVT200) to 180 ° (50 wt%). The wettability of the steel surface goes from being hydrophilic to hydrophobic at 30 wt% concentration of Eicosane. This means that the attraction force between oil and steel is higher than that between water and steel achieved by pre-wetting of the steel with the wax. So the water is repelled by the oil phase. The higher the concentration of paraffins, the more hydrophobic the surface becomes, due to thicker and more uniform wax layer on the steel surface.

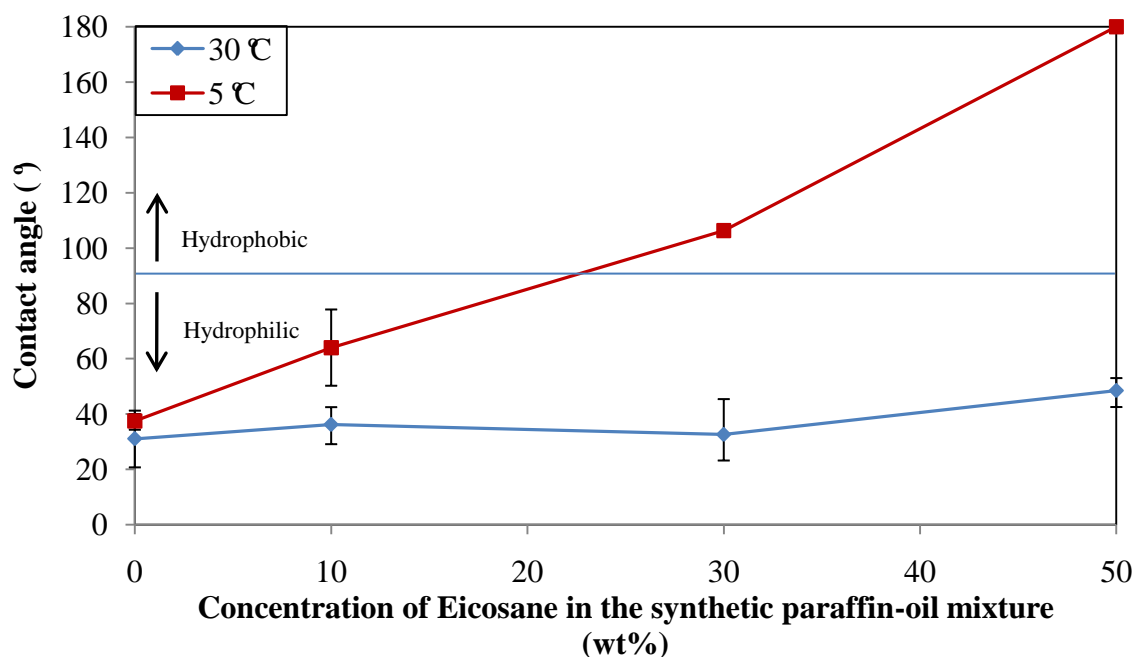


Figure 28. Contact angle measurements of the droplets of the synthetic paraffin-oil mixture in 1 wt% NaCl aqueous solution (water) phase at 5 °C and 30 °C on the surface of carbon steel (X65) which is pre-wetted with the synthetic paraffin-oil mixture.

3.4.3 Water droplet in oil phase

Figure 29 shows images of contact angle measurements for water droplets in synthetic paraffin-oil mixture at different concentrations of Eicosane at 30 °C. Each image is assigned a label with the composition of oil phase environment surrounding the water droplet and the contact angle between the water droplet and specimen surface.

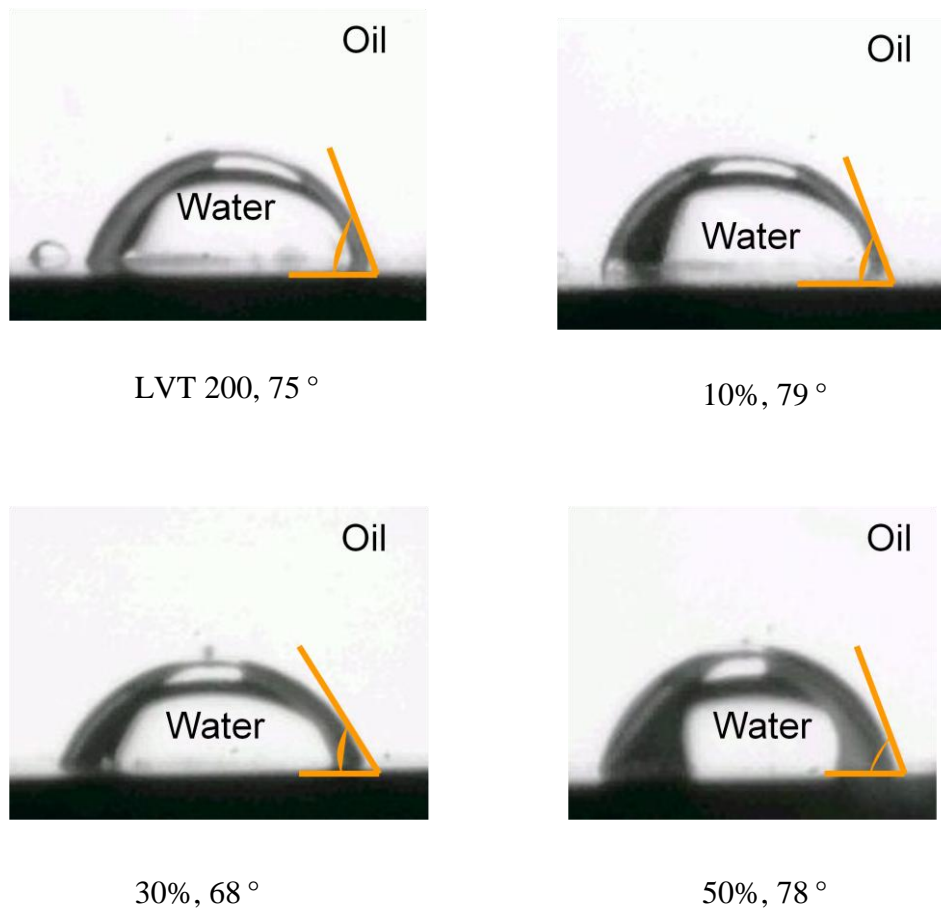
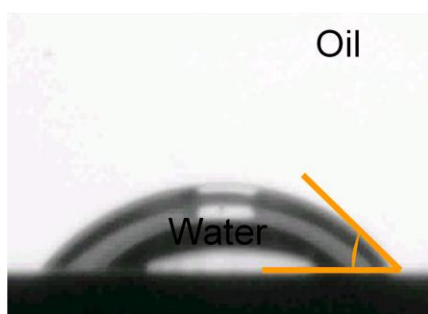


Figure 29. Water droplets on the surface of the carbon steel (X65) in the synthetic paraffin-oil mixture at 30 °C.

Because the synthetic paraffin-oil mixture is solid below the WAT (5 °C), the contact angle measurements cannot be conducted. *Figure 30* only shows images of contact angle measurements for water droplets in LVT200 oil phase at 5 °C. Under the image, a label is showed the composition of oil environment (LVT200) and the contact angle between the water droplet and specimen surface.



LVT 200, 59 °

Figure 30. Water droplets on the surface of the carbon steel (X65) in LVT200 oil phase at 5 °C.

Figure 31 shows the plot of contact angle measurements for synthetic paraffin-oil mixture droplets in synthetic paraffin-oil mixture at different concentrations of Eicosane at 5 °C and 30 °C. From *Figure 31*, when the temperature is 30 °C (above the WAT), contact angles of synthetic paraffin-oil mixtures at 4 different concentrations of Eicosane are the same and close to 75°. When the temperature is 5 °C (below the WAT), the LVT200 droplet is 59°. The steel surface is hydrophilic at both 30 °C (above the WAT) and 5 °C (below the WAT). This means that the contact angle does not change with the addition of paraffins (Eicosane) when the temperature is 30 °C (above the WAT), which implies that the addition of paraffins should not affect the wettability of the steel surface,

which continues to be hydrophilic. This is in good agreement with results in Section 3.4.1 which shows the oil droplet in water phase at both 30 °C (above the WAT) and 5 °C (below the WAT).

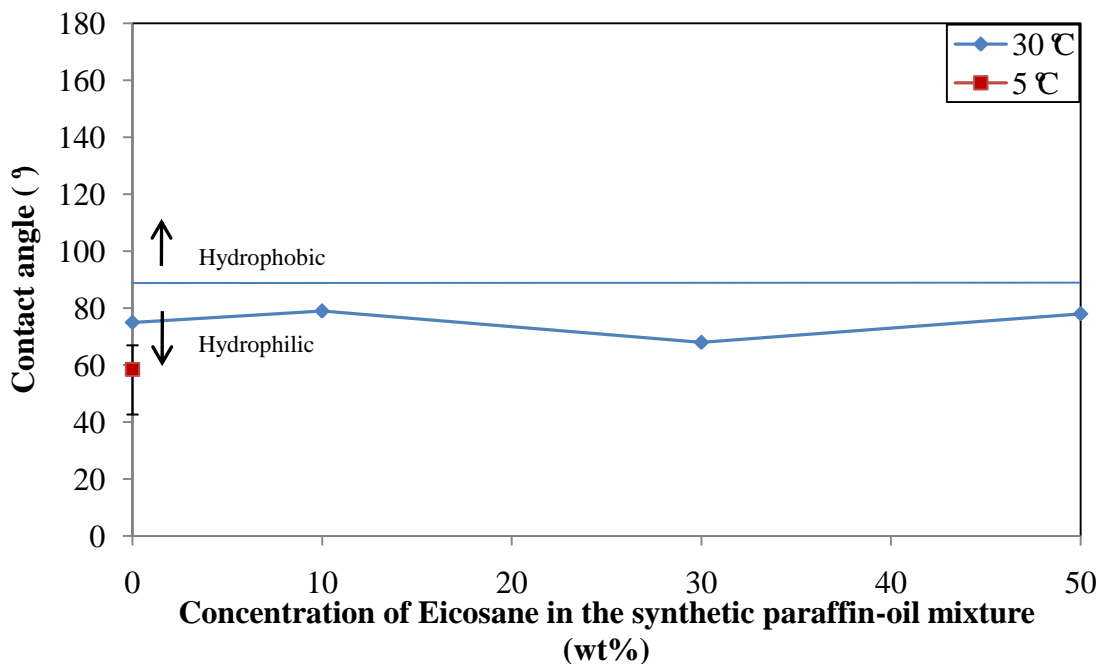


Figure 31. Contact angle measurements of water droplets in the synthetic paraffin-oil mixture at 5 °C and 30 °C.

3.4.4 Water droplet in oil phase (oil pre-wet specimen)

Figure 32 shows images of contact angle measurements for water droplets in LVT oil phase at 30 °C when carbon steel (X65) specimen is pre-wetted with different concentrations of Eicosane in synthetic paraffin-oil mixture. Each image is labeled with the composition of the pre-wetted layer on the specimen and the contact angle between the water droplet and specimen surface.

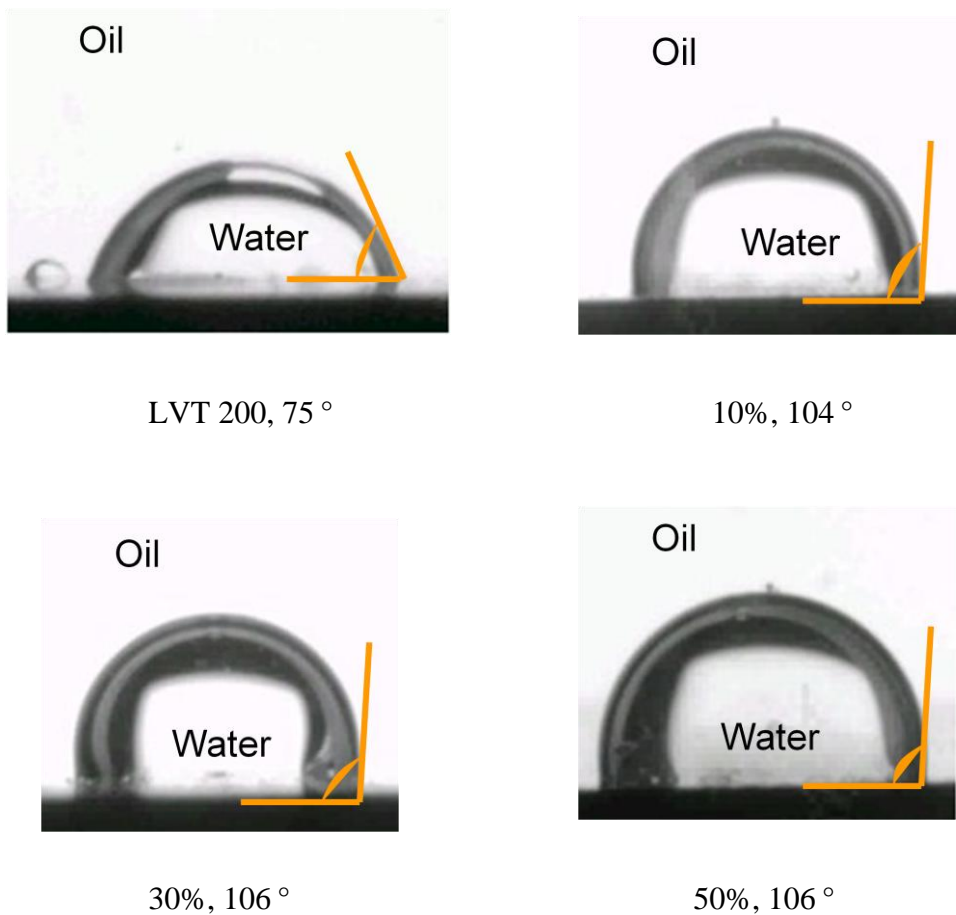


Figure 32. Water droplets in the synthetic paraffin-oil mixture at 30 °C on the surface of carbon steel (X65) which is pre-wetted with the synthetic paraffin-oil mixture.

For the measurements at a temperature below the WAT (5 °C), the LVT200 was used instead of synthetic paraffin-oil mixture as the oil phase, because the synthetic paraffin-oil mixture is solid below the WAT. *Figure 33* shows images of contact angle measurements for water droplets in LVT200 oil phase at 5 °C when carbon steel (X65) specimen is pre-wetted by different concentration mixtures of Eicosane in synthetic

paraffin-oil. Each image is labeled with the composition of pre-wetted layer on the specimen and the contact angle between the water droplet and specimen surface.

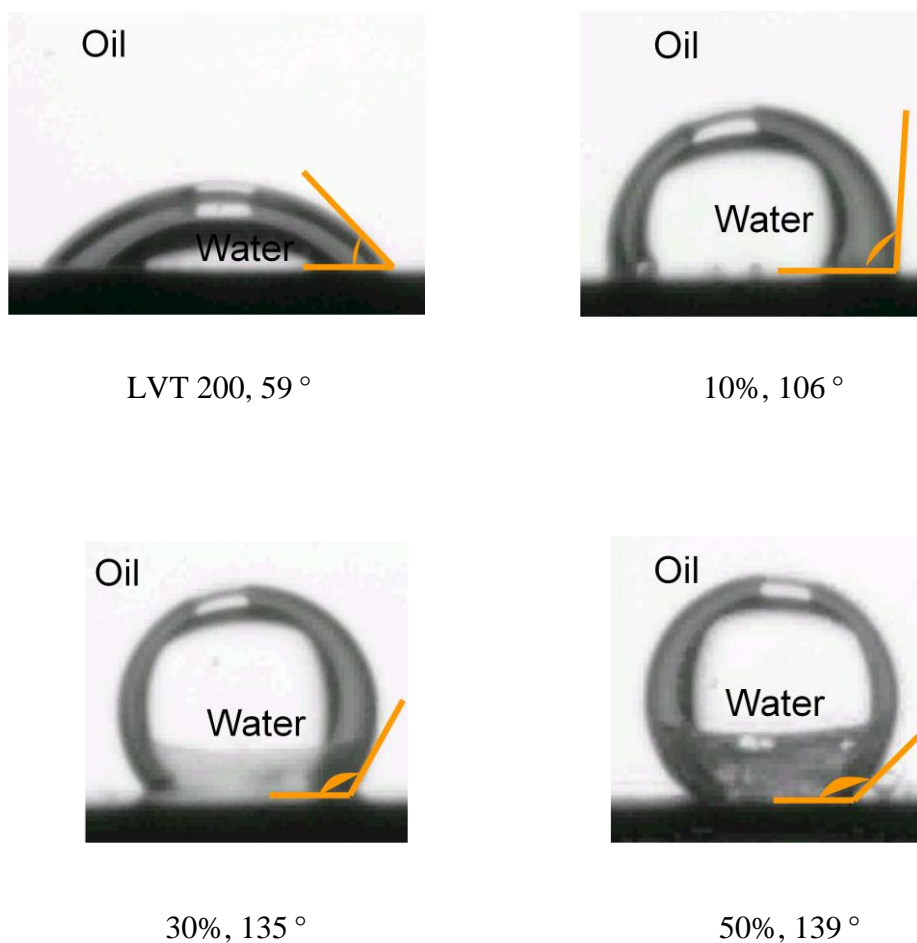


Figure 33. Water droplet in LVT200 oil phase at 5 °C on the surface of carbon steel (X65) which is pre-wetted with the synthetic paraffin-oil mixture.

Figure 34 shows the results of the contact angle measurements of water droplets in LVT200 oil phase with the carbon steel (X65) specimen pre-wetted with different concentrations of Eicosane in synthetic paraffin-oil mixture at 5 °C and 30 °C. When the

temperature is below the WAT the contact angle changes significantly from 59 °(LVT200) to 139 ° (50 wt%). The wettability is changed significantly from hydrophilic to hydrophobic at 10 wt% concentration of Eicosane. This also happened when the temperature is above the WAT, but was not as pronounced. This is in good agreement with results in Section 3.4.2 suggesting that when the steel surface is covered by a wax layer, the surface will remain hydrophobic.

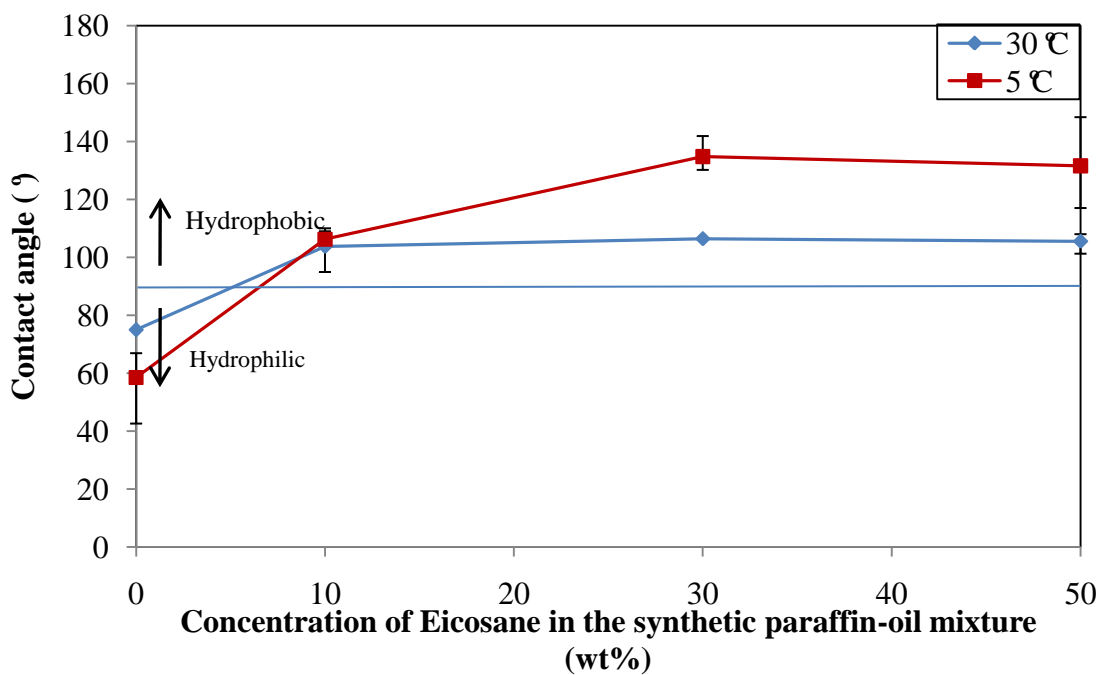


Figure 34. Contact angle measurements of water droplets in the synthetic paraffin-oil mixture at 5 °C and 30 °C on the surface of carbon steel (X65) which is pre-wetted with the synthetic paraffin-oil mixture.

3.5 Interfacial tension

A tensiometer is employed to measure interfacial tension, which is an important parameter affecting flow patterns. The procedure for the measurement is described in Section 2.5, and Table 8 (page 48) shows the test matrix.

Figure 35 shows the comparison of interfacial tension of synthetic paraffin-oil mixtures at 30 °C. It can be seen that the oil-water interfacial tension of different concentration paraffins are the same (45 dyne/cm), which means that the addition of paraffins did not affect the transition between stratified or dispersed flow in oil-water flow. This is because no paraffin has accumulated at the oil-water interface.

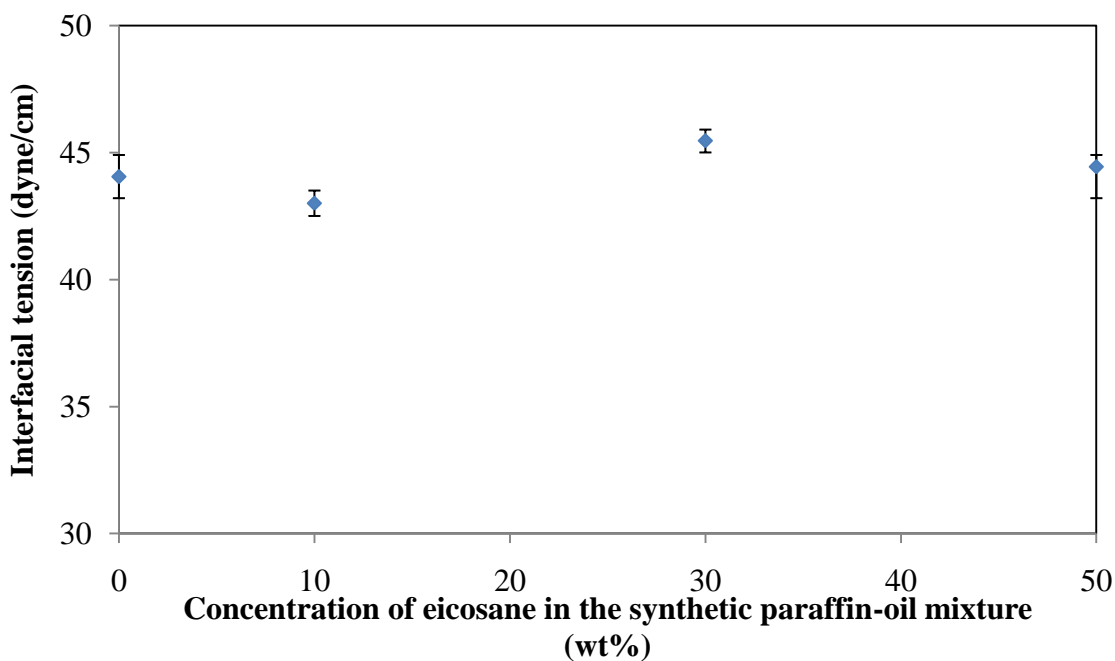


Figure 35. Interfacial tension measurements between the synthetic paraffin-oil mixture and 1 wt% NaCl aqueous solution at 30 °C.

CHAPTER 4: THERMODYNAMIC MODEL FOR WAX PRECIPITATION

During oil production and transportation, three practical methods are conventionally employed to avoid wax precipitation which would otherwise cause blockage of the pipeline. “Pigging” is a method in which a “pig” is used to prevent wax buildup. Pigs are large plugs that are inserted into and travel throughout the pipeline driven by flows and originally developed to remove deposits through a pipeline. Heating/thermal insulation of the pipelines is another frequently used method, but it can only be employed effectively when the distance of transportation is short. Recently, a chemical formulation called “wax inhibitor” has been developed to prevent precipitation of wax. These three methods can be used in the field to solve the wax precipitation to a great extent. Both the positive (corrosion protection) and negative (pipeline plugging) effects of wax deposition are more easily managed if the WAT of the crude oil can be predicted before it is produced and transported. In this chapter, a thermodynamic model for wax precipitation is compiled in order to predict the occurrence of the wax appearance temperature (WAT).

In a paraffinic oil system, three-phase (solid, liquid and vapor) equilibria can be formulated. The thermodynamic models proposed in the literature are typically based on the three-phase equilibria. Only the liquid-solid equilibrium (LSE) is considered as related to wax precipitation in the current project. There are two methods to study the liquid-solid equilibrium (LSE): the activity coefficient based model, such as Won’s model (1986, 1989), Hansen *et al.*’s model (1988) and Pederson *et al.*’s model (1991), and the cubic equation of state based models, such as Lira-Galeana *et al.*’s model (1996)

and Ji *et al.*'s model (2003). The current research employs the approach with activity coefficients to describe wax precipitation via liquid-solid equilibria (LSE), considering pressure range from low to moderate, and the temperature not far from ambient.

4.1 General solid-liquid equilibrium

When a system, which includes two phases (solid phase S and liquid phase L), comes to an equilibrium, the following statement can be made:

- 1) The temperatures (T) of both phases are equal.

$$T^S = T^L \quad (13)$$

- 2) The pressures (P) of both phases are equal.

$$P^S = P^L \quad (14)$$

- 3) The Gibbs free energies (G) of both phases are equal.

$$G^S = G^L \quad (15)$$

- 4) The fugacities (f) of the liquid and solid phases are equal.

$$f^S = f^L \quad (16)$$

Fugacity is a measure of a chemical potential in the form of “adjusted pressure”. It reflects the tendency of a substance to prefer one phase (liquid, solid, or vapor) over another. Fugacity can be literally defined as “the tendency to flee or escape”, and has the same unit as pressure. The relationship between fugacity and Gibbs free energy is shown as follows (Sandler, 2006):

$$\frac{f^L}{f^S} = \exp\left(\frac{G^S - G^L}{RT}\right) \quad (17)$$

Therefore, Equation (16) can be obtained from Equation (15) by using the relationship between fugacity and Gibbs free energy (Equation (17)).

When the solid and liquid phases are in thermodynamic equilibrium, for a multi-component system, the fugacity f of component i in the solid (f_i^S), liquid (f_i^L) phases is the same.

$$f_i^L = f_i^S \quad (18)$$

For a non-ideal, multi-component system, the fugacity in the solid phase, based on the solid solution theory, which assumes that all the components in the solid phase are miscible in all proportions, is expressed via

$$f_i^S = r_i^S x_i^S f_{i,pure}^S = r_i^S x_i^S f_{i,pure}^{oS} \exp\left(\int_{P_0}^P \frac{V_i^S}{RT} dP\right) \quad (19)$$

where r_i^S is the activity coefficient of component i in solid phase, x_i^S is the molar fraction of component i in solid phase, $f_{i,pure}^S$ is the fugacity of pure component i at the same state (T and P) as f_i^S , $f_{i,pure}^{oS}$ is the fugacity of pure component i at the reference pressure P_0 , V_i^S is the partial molar volume of component i in solid phase, R is the gas constant, P is the pressure and T is the temperature.

Similarly, the fugacity in the liquid phase is

$$f_i^L = r_{i,pure}^L x_i^L f_{i,pure}^L = r_{i,pure}^L x_i^L f_{i,pure}^{oL} \exp\left(\int_{P_0}^P \frac{V_i^L}{RT} dP\right) \quad (20)$$

where r_i^L is the activity coefficient of component i in liquid phase, x_i^L is the molar fraction of component i in liquid phase, $f_{i,pure}^L$ is the fugacity of pure component i at the same state (T and P) as f_i^L , $f_{i,pure}^{oL}$ is the fugacity of pure component i at the reference pressure P_0 , and V_i^L is the partial molar volume of component i in liquid phase.

Combining Equations (18), (19) and (20), we obtain the expression for the solid-liquid equilibrium coefficient K_i^{SL} :

$$K_i^{SL} = \frac{x_i^S}{x_i^L} = \frac{r_i^L f_{i,pure}^{oL}}{r_i^S f_{i,pure}^{oS}} \exp\left(\int_{P_0}^P \frac{V_i^L - V_i^S}{RT} dP\right) \quad (21)$$

The exponential term on the right-hand side of Equation (21) represents the pressure dependence, since the difference between the partial molar volumes of liquid and solid, V_i^L and V_i^S , is considered small at low to moderate pressure (Won, 1989, Pedersen *et al.*, 1991), the exponential term in Equation (21) is neglected, and K_i^{SL} can be expressed as:

$$K_i^{SL} = \frac{x_i^S}{x_i^L} = \frac{r_i^L f_{i,pure}^{oL}}{r_i^S f_{i,pure}^{oS}} \quad (22)$$

In Equation (22), the solid-liquid equilibrium coefficient K_i^{SL} is expressed as the product of two terms: the first term, $\frac{r_i^L}{r_i^S}$, characterizes the non-ideality of the liquid and solid solutions, and the second term, $\frac{f_{i,pure}^{oL}}{f_{i,pure}^{oS}}$, can be determined from the change of Gibbs free energy between the pure solid and pure liquid at the reference state.

4.2 Fugacities of pure substance for liquid and solid at the reference state

According to Pederson *et al.* (1991), the ratio of standard state fugacities at temperature T and pressure P_0 of pure component i in the liquid and solid phases, can be related to the change in Gibbs free energy change:

$$\frac{f_{i,pure}^{oL}}{f_{i,pure}^{oS}} = \exp\left(\frac{\Delta G_{tr}}{RT}\right) \quad (23)$$

where ΔG_{tr} is the molar change in Gibbs free energy associated with the transition of pure component i from solid (wax) to liquid state form at temperature T and pressure P_0 .

To calculate the ΔG_{tr} , the following general thermodynamic relation is used:

$$\Delta G = \Delta H - T\Delta S \quad (24)$$

where ΔG is the Gibbs free energy change, ΔH is the enthalpy change, and ΔS is the entropy change.

For a pure component i in solid phase, the solid-liquid transition usually takes place at normal melting temperature (T^m). The heat liberated from this transition is equal to heat of melting (ΔH_i^m). For a pure substance such as a normal paraffin, the heat (or enthalpy) of melting at the normal melting temperature can be obtained from experimental data.

Therefore, the enthalpy change (ΔH_{tr}) for pure substance, associated with a solid-liquid phase transition at a temperature T lower than T^m , can be presented as

$$\Delta H_{tr} = \Delta H^m \quad (25)$$

where ΔH^m is the heat of melting.

Similarly, entropy change (ΔS_{tr}) for pure substance associated with the solid-liquid transition can be derived as follows:

$$\Delta S_{tr} = \frac{\Delta H^m}{T^m} \quad (26)$$

By combining Equations (23)-(26), the following expression can be derived for the ratio between the standard state fugacities of pure component i in the liquid phase and in the solid phase.

$$\frac{f_{i,pure}^{oL}}{f_{i,pure}^{oS}} = \exp\left(\frac{\Delta H_i^m}{RT} \left(1 - \frac{T}{T_i^m}\right)\right) \quad (27)$$

Normal melting temperature (T_i^m) and heat of melting (ΔH_i^m) can be measured experimentally and looked up in tables.

Won (1989) employed the following correlations for normal paraffins, based on experimental data which relate the melting properties of normal paraffins to their molecular weight in order to calculate ΔH_i^m (cal/mol) and T_i^m (K).

$$\Delta H_i^m = 0.1426 \times m_i \times T_i^m \quad (28)$$

$$T_i^m = 374.5 + 0.02617 \times m_i - 20172/m_i \quad (29)$$

where m_i is the molecular weight of component i .

Combining Equations (22) and (27), the following equation can be derived:

$$K_i^{SL} = \frac{x_i^S}{x_i^L} = \frac{r_i^L}{r_i^S} \exp\left(\frac{\Delta H_i^f}{RT} \left(1 - \frac{T}{T_i^f}\right)\right) \quad (30)$$

Therefore, the solid-liquid equilibrium coefficient K_i^{SL} is only related to the melting properties of pure components and the ratio of activity coefficients.

4.3 Activity coefficient model

Won (1989) used regular solution theory to calculate the activity coefficients r_i^L and r_i^S , which are determined from the solubility parameters δ_i^L and δ_i^S of the individual components.

$$\ln r_i^L = \frac{V_i^L (\bar{\delta}^L - \delta_i^L)^2}{RT} \quad \ln r_i^S = \frac{V_i^S (\bar{\delta}^S - \delta_i^S)^2}{RT} \quad (31)$$

$$\bar{\delta}^L = \sum_i \Phi_i^L \delta_i^L \quad \bar{\delta}^S = \sum_i \Phi_i^S \delta_i^S \quad (32)$$

$$\Phi_i^L = \frac{x_i^L V_i^L}{\sum_i x_i^L V_i^L} \quad \Phi_i^S = \frac{x_i^S V_i^S}{\sum_i x_i^S V_i^S} \quad (33)$$

where δ_i^L and δ_i^S are the solubility parameters of component i in liquid and solid phase, respectively, Φ_i^L and Φ_i^S are the volume fraction of component i in liquid and solid phase, respectively, and $\bar{\delta}^L$ and $\bar{\delta}^S$ are the mean solubility parameters in liquid and solid phase, respectively.

Combining Equations (31)-(33), we get

$$\frac{r_i^L}{r_i^S} = \exp\left(\frac{V_i}{RT} \left((\bar{\delta}^L - \delta_i^L)^2 - (\bar{\delta}^S - \delta_i^S)^2 \right)\right) \quad (34)$$

Won (1986) gave the values of the solubility parameters for normal paraffins, which are cited in Table 9.

Table 9. Values of Solubility Parameters for Normal Paraffins (Won, 1986)

Type of paraffins	δ_i^L (cal/cc) ^{0.5}	δ_i^S (cal/cc) ^{0.5}	Type of paraffins	δ_i^L (cal/cc) ^{0.5}	δ_i^S (cal/cc) ^{0.5}
n-C1	5.68	5.68	n-C21	8.11	10.1
n-C2	6.6	6.6	n-C22	8.13	10.1
n-C3	6.65	6.65	n-C23	8.15	10.1
n-C4	6.65	6.65	n-C24	8.17	10.2
n-C5	7.02	7.62	n-C25	8.18	10.2
n-C6	7.25	8.13	n-C26	8.2	10.3
n-C7	7.41	8.5	n-C27	8.21	10.3
n-C8	7.53	8.78	n-C28	8.22	10.3
n-C9	7.63	9	n-C29	8.24	10.3
n-C10	7.71	9.17	n-C30	8.25	10.4
n-C11	7.78	9.32	n-C31	8.26	10.4
n-C12	7.83	9.44	n-C32	8.27	10.4
n-C13	7.88	9.55	n-C33	8.28	10.4
n-C14	7.92	9.64	n-C34	8.29	10.4
n-C15	7.96	9.72	n-C35	8.3	10.5
n-C16	7.99	9.79	n-C36	8.31	10.5
n-C17	8.02	9.86	n-C37	8.32	10.5
n-C18	8.05	9.92	n-C38	8.33	10.5
n-C19	8.07	9.97	n-C39	8.34	10.5
n-C20	8.09	10	n-C40	8.35	10.6

The partial molar volume (cm³/mol) of component *i* can be calculated using the following correlations proposed by Won (1989):

$$V_i = V_i^L = V_i^S = \frac{m_i}{d_{i,25}^L} \quad (35)$$

where $d_{i,25}^L$ is the liquid phase density (g/cm^3) of component i at 25 °C (298K). It can be calculated by the following equation, which is applicable to normal paraffins:

$$d_{i,25}^L = 0.8155 + 0.6272 \times 10^{-4} \times m_i - \frac{13.06}{m_i} \quad (36)$$

Combining Equations (30) and (34), the ratio between the mole fractions of component i in the solid (wax) phase and in the liquid phase can be derived as

$$K_i^{SL} = \frac{x_i^S}{x_i^L} = \exp\left(\frac{V_i}{RT} \left((\bar{\delta}^L - \delta_i^L)^2 - (\bar{\delta}^S - \delta_i^S)^2 \right) + \frac{\Delta H_i^f}{RT} \left(1 - \frac{T}{T_i^f} \right)\right) \quad (37)$$

The ratio of activity coefficient $\frac{r_i^L}{r_i^S}$ characterizes the non-ideality of liquid and solid solutions, and for ideal system, it can be assumed to be 1. The system can be treated as ideal if the oil mixture is composed exclusively of normal paraffins, at normal condition, meaning that the pressure ranges from low to moderate and the temperature is ambient.

Based on this assumption ($\frac{r_i^L}{r_i^S} = 1$), Equation (37) can be simplified to:

$$K_i^{SL} = \frac{x_i^S}{x_i^L} = \exp\left(\frac{\Delta H_i^f}{RT} \left(1 - \frac{T}{T_i^f} \right)\right) \quad (38)$$

Therefore, in Equation (37), the solid-liquid equilibrium coefficient K_i^{SL} relates solely to the melting properties of the pure components, which can be evaluated using the molecular weight correlations (Equations (28) and (29)).

4.4 Modeling calculation

The mass balance for the overall process in the system is

$$F = L + S \quad (39)$$

where F, L and S stand for the mole of feed, liquid phase and solid phase, respectively.

The mass balance for each component i can be expressed as

$$F x_i = L x_i^L + S x_i^S \quad (40)$$

where x_i is the feed molar fraction of component i in the system, x_i^L is the molar fraction of component i in liquid phase, and x_i^S is the molar fraction of component i in solid phase.

By combining Equations (21), (39) and (40), we can derive

$$x_i^L = \frac{x_i}{1 + (K_i^{SL} - 1) \frac{S}{F}} \quad (41)$$

$$x_i^S = K_i^{SL} x_i^L \quad (42)$$

where Equation (42) is the rearrangement of Equation (21).

The sum of molar fraction of component i in liquid phase is 1.

$$\sum x_i^L = 1 \quad (43)$$

By combining Equation (41) and (43), the following equation can be achieved:

$$\sum \frac{x_i}{1 + (K_i^{SL} - 1) \frac{S}{F}} = 1 \quad (44)$$

Therefore, by knowing the values of K_i^{SL} , we can calculate $\frac{S}{F}$ in Equation (44).

Consequently, x_i^L and x_i^S in Equations (41) and (42) can be calculated.

It should be noted that if Equation (43) is satisfied, we can get the conclusion that the sum of molar fraction of component i in solid phase is 1 automatically according to mass balance.

At a given temperature, the wax solid which precipitates from crude oil can be expressed as:

$$\text{Wax weight (\%)} = \frac{\text{Total precipitated mass}}{\text{Mass of crude oil}} \times 100 = \frac{\sum\{m_i x_i^S (\frac{S}{F})\}}{\sum(m_i x_i)} \times 100 \quad (45)$$

The algorithm for this wax precipitation model is expressed as follows.

1. Input the feed specifications of the oil mixture including x_i and m_i .
2. Calculate the melting properties (T_i^m and ΔH_i^m) in Equations (28) and (29).
3. Calculate the values of K_i^{SL} in Equation (38).
4. Calculate the molar fraction distribution value $\frac{S}{F}$ in Equation (44).
5. Calculate the values of x_i^L and x_i^S in Equations (41) and (42).
6. Calculate the wax weight (%) in Equation (45).

The detailed procedure chart (*Figure 36*) is described below.

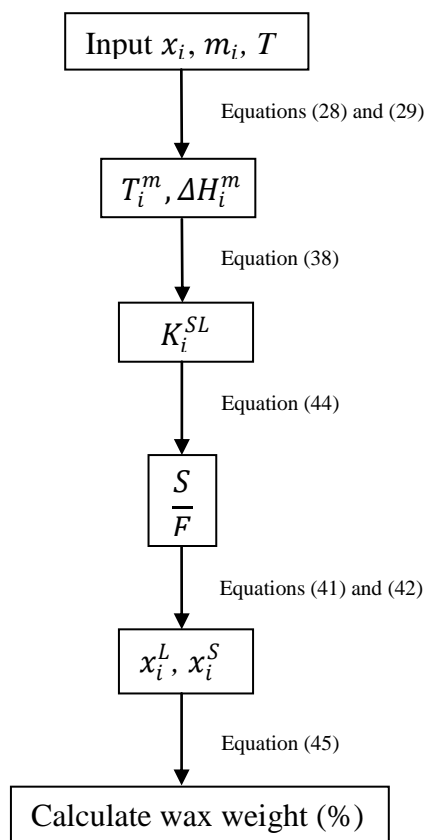


Figure 36. Procedure chart of the calculation of thermodynamic model for wax precipitation.

4.5 Model validation

Three synthetic mixtures of different compositions of normal paraffins system are chosen to validate the thermodynamic model for wax precipitation. Table 10 shows the specifications of these synthetic mixtures, which were presented by Pauly *et al.* (1998).

Table 10. *Composition of the Synthetic Oil Mixtures Used to Test the Model (Pauly et al., 1998)*

Feed composition	Mass%		
	Mixture A	Mixture B	Mixture C
n-C10	64.73	47.76	65.02
n-C18	0	7.17	3.55
n-C19	0	6.41	3.55
n-C20	10.30	5.74	3.56
n-C21	7.40	5.16	3.55
n-C22	5.29	4.63	3.53
n-C23	3.79	4.16	3.51
n-C24	2.70	3.72	3.48
n-C25	1.93	3.32	3.45
n-C26	1.37	2.97	3.41
n-C27	0.97	2.64	3.39
n-C28	0.69	2.08	0
n-C29	0.49	1.85	0
n-C30	0.35	2.39	0

Figures 37-39 show the results for the amount of wax precipitation calculated using the model compared to the experimental results.

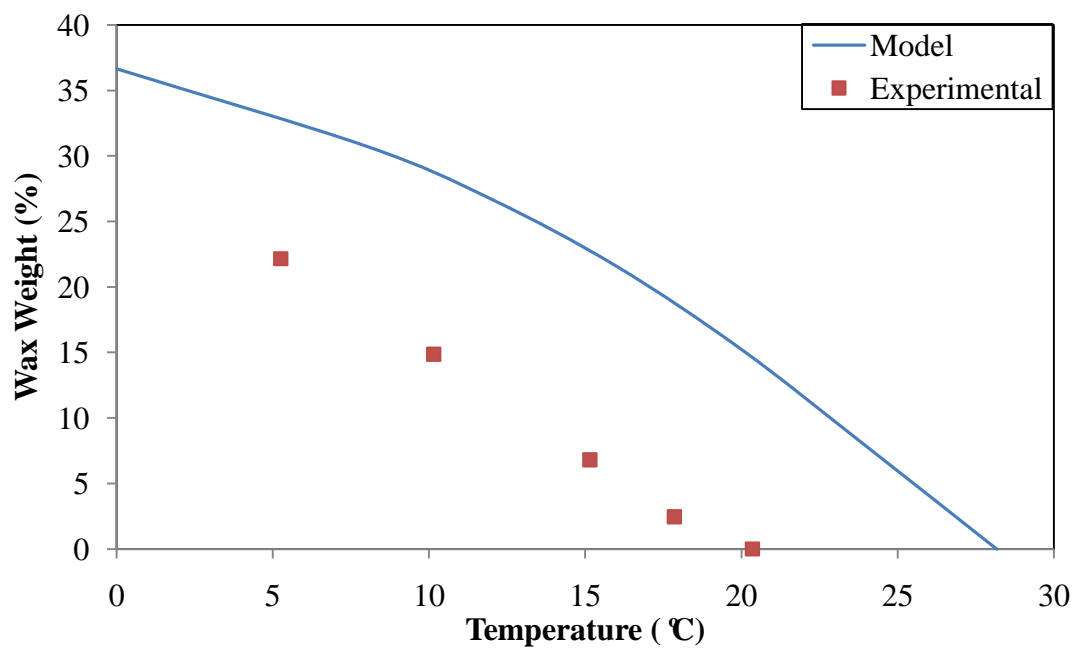


Figure 37. Experimental and predicted wax precipitation results for synthetic Mixture A.

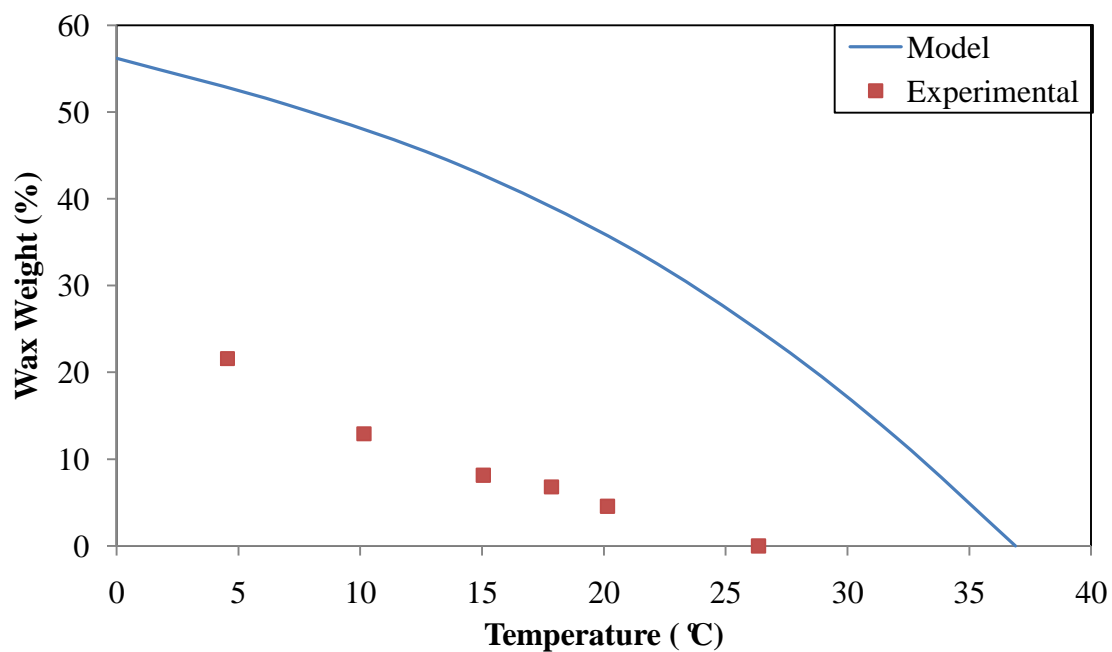


Figure 38. Experimental and predicted wax precipitation results for synthetic Mixture B.

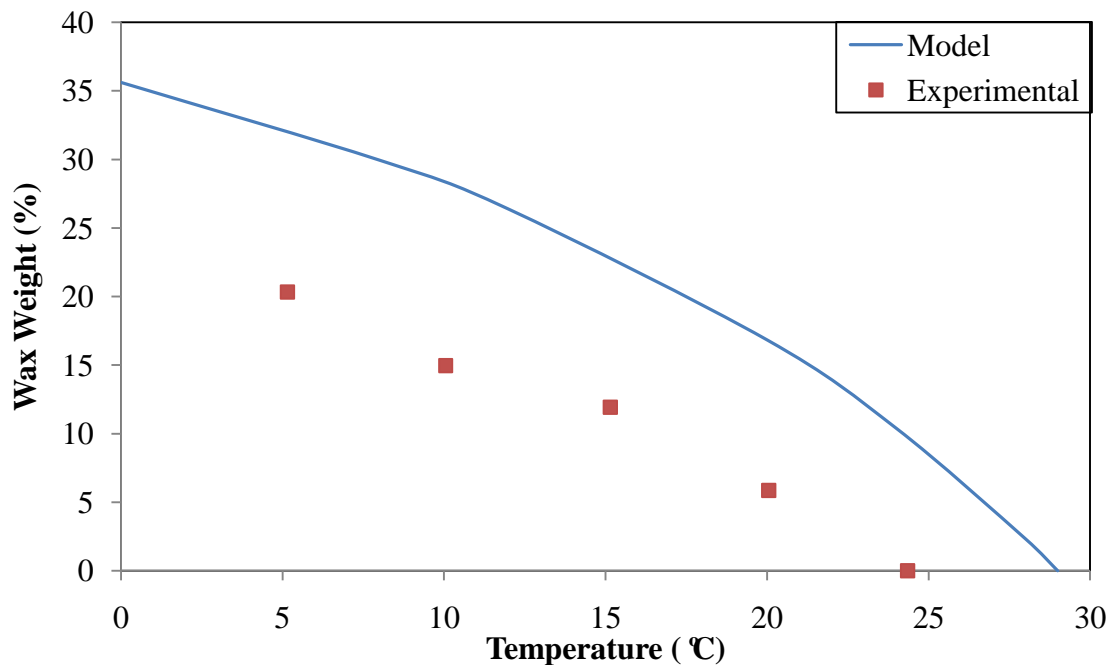


Figure 39. Experimental and predicted wax precipitation results for synthetic Mixture C.

When the temperature reaches the wax appearance temperature (WAT), the solid wax begins to precipitate. With further decreasing the temperature, more wax will precipitate. Therefore, in *Figures 37-39*, when the value on the vertical axis (Wax weight (%)) is 0, the corresponding value on the horizontal axis (Temperature (°C)) is the WAT.

As shown in the *Figures 37-39*, the trend of the predicted results is in good agreement with the experimental data in these synthetic normal paraffin mixtures, but an overestimation exists. Table 11 shows the comparison of the WAT between the experimental and the model results. The overestimation is due to the non-ideality of the mixtures, while the model was formulated for an ideal system. This needs improvement.

Table 11. Comparison of the WAT between Experimental and Model Results

Oil type	Experimental results (°C)	This model (°C)
Mixture A	21	29
Mixture B	27	37
Mixture C	25	29

At the end of section 4.3, an assumption that the ratio of activity coefficient is 1 ($\frac{r_i^L}{r_i^S} = 1$) for ideal mixture was made. However, this assumption is not appropriate because the mixture is not ideal. In the normal paraffin mixture, the more of the heavier components exist, the less ideal the mixture becomes, and hence the existence of heavier components causes the largest deviation from ideality. The ratio of activity coefficient should be different from 1 for heavier components in the normal paraffin mixture. Therefore, the assumption about the ratio of activity coefficient can be adjusted based on the activity coefficient model shown in Section 4.3.

The complicated theory and equations for calculating the ratio of activity coefficient $\frac{r_i^L}{r_i^S}$ can be simplified using Equations (31)-(33), (35) and (36) to obtain the following approximate equation:

$$\frac{r_i^L}{r_i^S} = \exp(Cm_i) \quad (46)$$

where now C is an arbitrary constant.

By adjusting the constant C , a value of -0.002 was found to fit better for the experimental data of all the mixtures. *Figure 40-42* show the new model results obtained by using Equation (46) for Mixtures A, B and C. It can be seen that the model lines are

now closer to the experimental data. Using Equation (46), the ratio of activity coefficient for each component becomes less than one. Moreover, the heavier the component is, the smaller ratio of activity coefficient becomes. For instance, the ratio of activity coefficient for C10 is 0.7 and for C30 is 0.43. This indicates that, by adjusting the ratio of activity coefficient, the effect of heavier components which makes the mixture move away from ideality is reduced. Therefore, the adjusted model agrees better with the experimental data than the original one.

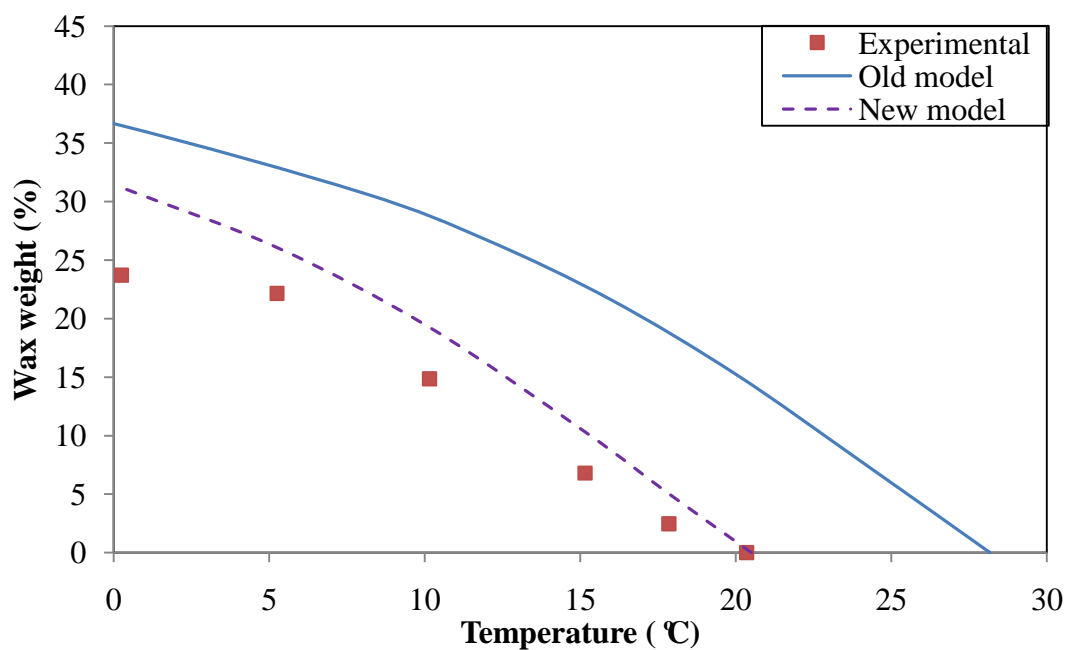


Figure 40. Wax precipitation results: experiments and new model conducted by adjusting the ratio of activity coefficient for Mixture A.

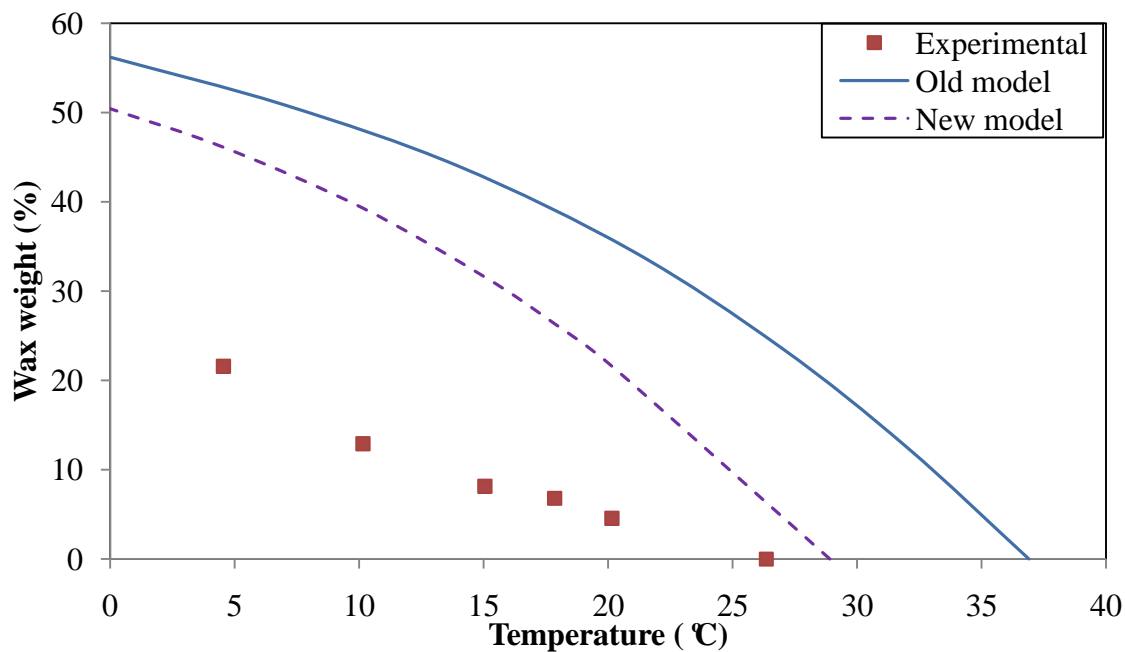


Figure 41. Wax precipitation results: experiments and new model conducted by adjusting the ratio of activity coefficient for Mixture B.

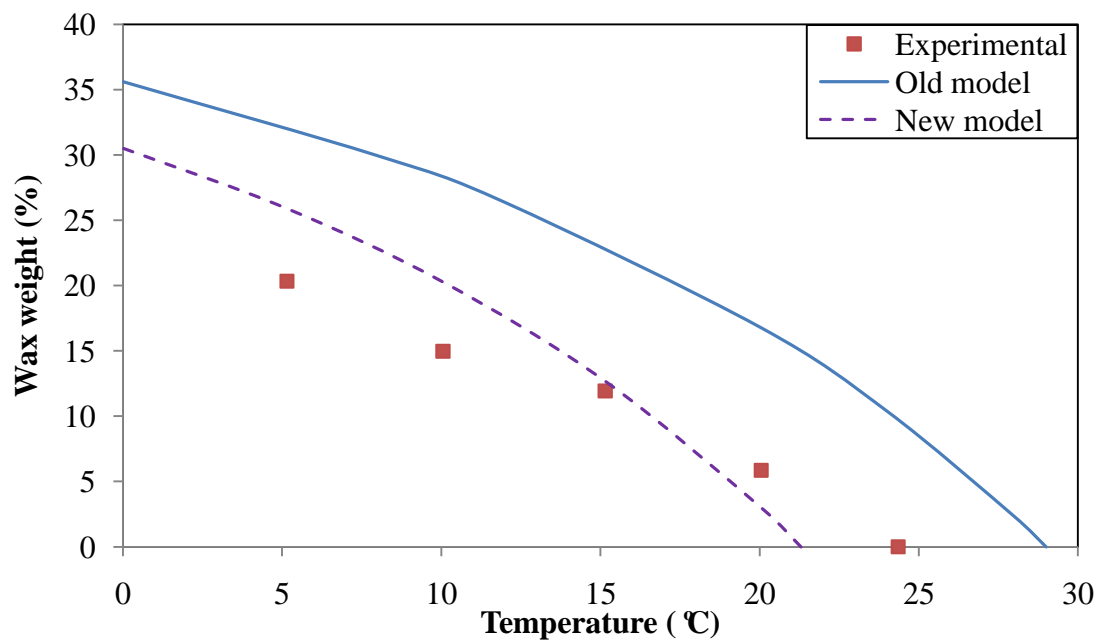


Figure 42. Wax precipitation results: experiments and new model conducted by adjusting the ratio of activity coefficient for Mixture C.

CHAPTER 5: CONCLUSIONS

Based on the work performed in this research project, the following conclusions can be made.

- Paraffins produce significant corrosion inhibition at temperatures below the WAT by forming a wax layer on the steel surface. The corrosion inhibition is persistent with time.
- Paraffin wax layer on the steel surface can be removed at higher flow velocity.
- The mechanism of paraffins formation on steel surface is a physi-sorption.
- When the temperature is below the WAT, paraffin wax on steel surface changes the surface wettability from hydrophilic to hydrophobic.
- Paraffins should not affect the flow pattern at temperatures above the WAT as they do not affect the water/oil interfacial tension.
- A simple ideal thermodynamic model for predicting wax precipitation is formulated showing a significant overestimation of WAT. The overestimation was reduced by adjusting the ratio of activity coefficient based on a simplified activity coefficient model.

REFERENCES

- Ajmera, P. (2009). Effect of Asphaltene on phase wetting and internal corrosion in oil-water two phase flow. *MS thesis, Ohio University*.
- Berg, J. C. (1993). *Wettability*. New York: Marcel Dekker, Inc.
- Cai, J., Nestic, S., & de Waard, C. (2004). Modeling of water wetting in oil-water pipe flow. *NACE 2004, Paper No.04663*, 1-19.
- Cai, J., Li, C., Tang, X., Ayello, F., & Nestic, S. (2005). Water wetting and CO₂ corrosion in horizontal & inclined oil-water pipe flows. *Institute for Corrosion and Multiphase Technology, Ohio University*, final water wetting project report to Saudi Aramco Oil Company.
- Cost of Corrosion. <http://corrosioncost.com/>
- Coutinho, J. A. P., Pauly, J., & Daridon, J. L. (2001). A Thermodynamic model to predict wax formation in petroleum fluids. *Brazilian Journal of Chemical Engineering*, 18(4).
- CSC Scientific Company. <http://www.cscscientific.com/>
- dos Santos, R. G., Mohamed, R. S., Bannwart, A. C., & Loh, W. (2006). Contact angle measurements and wetting behavior of inner surfaces of pipelines exposed to heavy crude oil and water. *Journal of Petroleum Science & Engineering*, 51, 9-16.
- Efird, K.D., & Jasinki, R. J. (1989). Effect of the crude oil on corrosion of steal in crude oil/brine production. *Corrosion Engineering* 45 (2), 165-171.

- Hansen, J. H., Fredenslund, A., Pederson, K. S., & Ronningsen, H. P. (1988). A thermodynamic model for predicting wax formation in crude oils. *AIChE Journal*, 34 (12), 1937-1942.
- Hernandez, S. E., & Nesic, S. (2005). Use of artificial networks for predicting crude oil effect on CO₂ corrosion of carbon steel. *NACE Corrosion 2005*, paper no. 05554.
- Ji, H. (2003). Wax phase equilibria: developing a thermodynamic model using a systematic approach. *Fluid Phase Equilibria*, 216, 201-217.
- Jones, D. A. (1996). *Principles and prevention of corrosion*, 2nd ed. Upper Saddle River, NJ: Prentice-Hall, Inc.
- Li, C., Tang, X., Ayello, F., Nesic, S., & Khamis, J. N. (2006). Experimental study on water wetting and CO₂ corrosion in oil-water two-phase flow. *Corrosion/2006* Paper no. 06595. NACE International, Houston, Texas.
- Lira-Galeana, C., Firoozabadi, A., & Prausnitz, J. M. (1996). Thermodynamics of wax precipitation in petroleum mixtures. *AIChE Journal*, 42 (1), 239-248.
- Morales, J. L., Perdomo, J. J., Ramirez, M., & Vilorio, A. (2000). Effect of crude oil contaminants on the internal corrosion in gas pipelines. *NACE Corrosion 2000*, paper no. 00040.
- MSDS provided by Penreco Company.
- [http://www.littleredservices.com/FieldDocs/MSDS/Mineral Oil- Penreco LVT 200.pdf](http://www.littleredservices.com/FieldDocs/MSDS/Mineral%20Oil-Penreco%20LVT%2000.pdf)
- Nesic, S. (2007). Key issues related to modeling of internal corrosion of oil and gas pipelines – a review. *Corrosion Science*, 49, 4308-4338.

- Nordsveen, M., Nestic, S., Nyborg, R., & Stangeland, A. (2003). A mechanistic model for carbon dioxide corrosion of mild steel in the presence of protective iron carbonate films – Part1: Theory and verification. *Corrosion*. 59(5), 443-456.
- Pauly, J., Dauphin, C., & Daridon, J. L. (1998). Liquid-solid equilibria in a decane + multi-paraffins system. *Fluid Phase Equilibria*, 149, 191-207.
- Pedersen, K. S., Skovborg, P., & Ronningsen, H. P. (1991). Wax precipitation from north sea crude oils. 4. Thermodynamic modeling. *Energy & Fuels*. 5 (6), 924-932.
- Reid, R. C., Prausnitz, J. M., & Poling, B. E. (1987). *The properties of gases & liquids*. 4th ed. Boston: McGraw-Hill.
- Rosen, M.J. (2004). *Surfactants and interfacial phenomena*. 3rd edition. NJ: John Wiley & Sons, Inc.
- Sandler, S. I. (2006). *Chemical, biochemical, and engineering thermodynamics*. 4th ed. NJ: John Wiley & Sons, Inc.
- Singh, P. (2000). Gel deposition of cold surfaces. *PhD dissertation*, University of Michigan.
- Speight, J. G. (1998). *The chemistry and technology of petroleum*. New York: Marcel Dekker Inc.
- Wikipedia. http://en.wikipedia.org/wiki/Thermoelectric_cooling/
- Won, K. W. (1986). Thermodynamics for solid solution-liquid-vapor equilibria - Wax phase formation from heavy hydrocarbon mixtures. *Fluid Phase Equilibria*, 30, 265-279.

Won, K. W. (1989). Thermodynamic calculation of cloud point temperatures and wax phase compositions of refined hydrocarbon mixtures. *Fluid Phase Equilibria*, 53, 377-396.

APPENDIX A: LINEAR POLARIZATION RESISTANCE

Linear polarization resistance (LPR), which is measured using a potentiostat, is a common electrochemical technique employed to measure the corrosion rate. The potentiostat polarizes the sample and records the resulting current and the polarization resistance is defined as the slope of the potential versus current density.

During the measurement, an open circuit potential delay is conducted until the open circuit potential remains stable. The steel specimen is polarized ± 5 mV around the open circuit potential at a scan rate of 0.125 mV/s. The polarization resistance can be converted to corrosion rate by the following equations:

$$i_{corr} = B \times \frac{1}{R_p} \times \frac{1}{A} \quad (\text{A.1})$$

where, i_{corr} is the corrosion current density in A/m², R_p is the polarization resistance in ohm, and A is the surface area of working electrode in m² (which is 5.4 cm² in this research). The proportionality constant B is calculated from the equation below.

$$B = \frac{\beta_a \beta_c}{2.303(\beta_a + \beta_c)} \quad (\text{A.2})$$

where, β_a and β_c are the anodic and cathodic Tafel slopes, which can be expressed as follows:

$$\beta_a = \frac{2.303RT}{\alpha_a F} \quad (\text{A.3})$$

$$\beta_c = \frac{2.303RT}{\alpha_c F} \quad (\text{A.4})$$

where, T is the absolute temperature in K, R is the universal gas constant (8.314 J/mol K), α_a and α_c are the symmetry factors for anodic and cathodic reactions, and F is Faraday's

constant (96,500 coulombs/equivalent). The values of α_a and α_c are typically 1.5 and 0.5, respectively (Jones, 1996).

Corrosion rate in mm/yr is calculated by the following equation.

$$CR = \frac{m}{At\rho} = \frac{i_{corr} M_w}{\rho nF} = 1.16i_{corr} \quad (\text{A.5})$$

where, m is the metal loss in kg, t is the test time in seconds, ρ is the density of the material in kg/m³, M_w is the molecular weight of iron in kg/mol, and n is the number of electrons exchanged in the electrochemical reaction.